Charge and current distribution in graphs

2003 J. Phys. A: Math. Gen. 36 12425

(http://iopscience.iop.org/0305-4470/36/50/005)

INSTITUTE OF PHYSICS PUBLISHING JOURNAL OF PHYSICS A: MATHEMATICAL AND GENERAL

J. Phys. A: Math. Gen. **36** (2003) 12425–12452 PII: S0305-4470(03)63631-0

Charge and current distribution in graphs

Christophe Texier[1,2] **and Pascal Degiovanni**[3]

[1] Laboratoire de Physique Théorique et Modèles Statistiques, Université Paris-Sud, Bât. 100, F-91405 Orsay Cedex, France
[2] Laboratoire de Physique des Solides, Université Paris-Sud, Bât. 510, F-91405 Orsay Cedex, France
[3] Laboratoire de Physique de l'ENS de Lyon (UMR CNRS 5672), École Normale Supérieure de Lyon, 46, allée d'Italie, 69364 Lyon Cedex 07, France

Received 19 May 2003
Published 2 December 2003
Online at stacks.iop.org/JPhysA/36/12425

Abstract
We consider graphs made of one-dimensional wires connected at vertices, and on which may live a scalar potential. We are interested in a scattering situation where such a network is connected to infinite leads. We study the correlations of the charge in such graphs out of equilibrium, as well as the distribution of the currents in the wires, inside the graph. These quantities are related to the scattering matrix of the graph. We discuss the case where the graph is weakly connected to the wires.

PACS numbers: 03.65.Nk, 73.23.−b

1. Introduction

Within the field of mesoscopic physics, the interest in graphs is motivated by the fact that they provide simple models for networks of wires, which are most of the time sufficient to describe the effect of interest (such as Aharonov–Bohm oscillations of the conductance of a ring, for example). Scattering theory plays a central role in mesoscopic physics: it provides a transparent formalism to study transport properties of phase coherent systems. Moreover, many other physical quantities can be related to scattering properties, such as the current noise [1, 2], the density of states through the Friedel sum rule, mesoscopic capacitance and relaxation resistance [3, 4]. Scattering on graphs has attracted the attention of many authors among which we can quote [5–14].

Despite the scattering matrix being a global quantity characterizing the full system, some local information can be extracted from it. This idea has been fruitfully exploited in many works of Büttiker *et al* (see review articles [15, 16] and references therein). To understand this point let us first consider the case of an isolated system (an isolated graph for example). In this case, the spectrum of the Schrödinger operator is discrete : $E_n, \varphi_n(x)$. Let us consider a physical quantity described by the operator $\hat{X}$, related to a conjugate variable f (that is $\hat{X} = (\partial/\partial f)\hat{H}$ where $\hat{H}$ is the Hamiltonian). Typical examples are provided by a

magnetization $\mathcal{M}$, a persistent current I, or the local density $\rho(x)$, which are conjugated to the magnetic field $-\mathcal{B}$, a flux[4] $-\phi$ and the potential $V(x)$, respectively. As is well known, a simple way to obtain the expectation value of the physical quantity of interest is to compute the derivative of the eigenenergies with respect to f : $X_n = \langle\varphi_n|\hat{X}|\varphi_n\rangle = \partial E_n/\partial f$. This result is known as the Feynman–Hellmann theorem.

A natural question is how to extend these relations to open systems that are connected to reservoirs possibly in an out-of-equilibrium situation. As is well known, the scattering approach will prove to be relevant for this purpose. The open system of interest in the present paper will be a graph connected to some infinite wires. In this case the spectrum is continuous. The stationary scattering states $\tilde{\psi}_E^{(\alpha)}(x)$ describing the injection of a plane wave at contact α provide the convenient basis of states for the discussion. Then we can relate the quantity of interest (that can give local information) to the scattering matrix Σ through the relation: $\langle\tilde{\psi}_E^{(\alpha)}|\hat{X}|\tilde{\psi}_E^{(\beta)}\rangle = -(1/2\mathrm{i}\pi)(\Sigma^\dagger\partial\Sigma/\partial f)_{\alpha\beta}$. In the case of graphs, this idea will be made explicit in three cases: (i) when $\hat{X} \to \hat{\rho}(x)$ is the local density of electrons[5] (then $f \to V(x)$ is the local potential), (ii) if $\hat{X} \to \hat{Q}$ is the charge of the graph ($f \to U$ is a potential constant inside the graph) and (iii) if $\hat{X} \to \hat{J}_{\mu\nu}$ is the current in an arc of the graph ($f \to \theta_{\mu\nu}$ is the flux along the arc).

The purpose of our paper is to study the distribution of charge and current densities in a graph out of equilibrium. The out of equilibrium regime is obtained by imposing different potentials at the external leads. A motivation for this study comes from the recent interest in quantum coherent devices such as Cooper pair boxes used for building charge qubits (see [20] for a review). The full spectrum of charge fluctuations is involved in the study of the dephasing in a qubit perturbed by the charge fluctuations of another conductor capacitively coupled to the first one [15, 21, 22]. In the same way, current density fluctuations are a source of dephasing for qubits based on flux states. Since the formalism developed in the present paper provides a systematic way of evaluating the charge and current density noise fluctuations in a mesoscopic circuit, it might be useful for estimating the dissipation and decoherence properties of some experimental systems of qubits. More precisely, it was shown that transition rates of a two-level system weakly coupled to a quantum environment are directly related to the unsymmetrized correlator: see for example [23] where the roles of the negative and positive parts of the spectrum of the unsymmetrized correlator are studied. On the other hand, the relaxation and decoherence rates are related to a symmetrized correlator [20]. Correlators are more directly accessible in noise measurements: in a recent work, Gavish *et al* [24, 25] proposed a description of the full measurement chain for the current noise of a mesoscopic sample. In this work, the unsymmetrized correlator is involved in excess noise measurement. Finally one should mention that experimentalists are now able, using photon-assisted tunnelling in a superconductor–insulator–superconductor tunnel junction, to measure the unsymmetrized current noise correlator in quantum mesoscopic devices [26]. The question of which correlator (symmetrized or not) to consider depends on the question of interest. Therefore we will consider in the following the unsymmetrized correlator as the fundamental object[6].

In this paper, electron–electron interactions will not be taken into account. However, even if this limits the applicability of our results, we recall that they can be taken into account in

[4] The variable conjugate to a flux line threading a loop of a planar graph is the current flowing through the semi-infinite line issuing from the flux [17] (see also [18]). This can also be easily understood in the two-dimensional plane [19].

[5] In this case $\langle\tilde{\psi}_E^{(\alpha)}|\hat{\rho}(x)|\tilde{\psi}_E^{(\beta)}\rangle = \tilde{\psi}_E^{(\alpha)*}(x)\tilde{\psi}_E^{(\beta)}(x)$ is an off-diagonal element of the local DoS [13, 15].

[6] There are indeed two unsymmetrized correlators depending on the order chosen. But for a system in a stationary regime, they can be simply related as shown in appendix A.

a mean-field Hartree approximation within the scattering approach, as has been developed in several papers by Büttiker and collaborators [3, 4, 27] (see also [28] for a review). In this framework the charge (or the current) contains two contributions: a bare contribution (injected charge) and a contribution from screening. Screening affects ac transport or finite frequency noise. It is not the purpose of our paper to consider such interaction effects; in other terms we will focus on the bare contribution of the charge and its relation to the scattering matrix of a graph.

This paper is organized as follows: first of all, the basic formalism [10] necessary for the discussion is recalled. Then the charge distribution inside the graph is analysed in detail. The first and second moments of the total charge are related to the scattering matrix. Finally analytic expressions for the full spectrum of charge fluctuations are provided.

In a further section we will show how currents inside the graph can be related to the scattering matrix. It was shown in [17] that the persistent current can be related to the derivative of the Friedel phase with respect to the magnetic flux. In this work the possible generalization to an out-of-equilibrium situation was not considered because the authors did not identify the different contributions of the various scattering states associated with the different leads. These contributions were identified later in [29]. Moreover, in Taniguchi's work, a formula relating the current–current correlations and the scattering matrix was proposed. Despite the contributions of the scattering states to the correlator being given, it is still not sufficient to study current–current correlations in an out-of-equilibrium situation (this point will be made clear later). Our results go beyond this limitation and provide a generalization of Taniguchi's result.

2. Basic formalism: scattering matrix

We consider the Schrödinger operator $-\mathrm{D}_x^2 + V(x)$ on a graph, where $\mathrm{D}_x = \mathrm{d}_x - \mathrm{i}A(x)$ is the covariant derivative (we choose units $\hbar = 2m = e = 1$). The graph is made of B bonds $(\alpha\beta)$, each being identified with an interval $[0, l_{\alpha\beta}] \in \mathbb{R}$. We call $x_{\alpha\beta}$ the coordinate that measures the distance from the vertex α. The Schrödinger operator acts on a scalar function $\varphi(x)$ which is described by B components $\varphi_{(\alpha\beta)}(x_{\alpha\beta})$, one for each bond. The bonds are connected at V vertices. The adjacency matrix $a_{\alpha\beta}$ encodes the structure of the graph: $a_{\alpha\beta} = 1$ if $(\alpha\beta)$ is a bond and $a_{\alpha\beta} = 0$ otherwise.

2.1. Vertex formulation

Let us first assume that the wavefunction is continuous at each vertex. This allows us to introduce vertex variables; we denote as $\varphi_\alpha \equiv \varphi(\alpha)$ the function at the vertex α. The continuity condition reads: $\varphi_{(\alpha\beta)}(x_{\alpha\beta} = 0) = \varphi_\alpha$ for all vertices β neighbours of α. A second condition is added to ensure current conservation at the vertices: $\sum_\beta a_{\alpha\beta}\mathrm{D}_x\varphi_{(\alpha\beta)}(x_{\alpha\beta} = 0) = \lambda_\alpha\varphi_\alpha$ where the sum over β runs over all neighbouring vertices of α due to the presence of the adjacency matrix. λ_α is a real parameter. The requirement of continuity of the wavefunction imposes a special scattering at the vertices: in particular, the transmission amplitudes of a plane wave of energy $E = k^2$ between two leads issuing from the same vertex of coordinance $m_\alpha = \sum_\beta a_{\alpha\beta}$ are all equal to $2/(m_\alpha + \mathrm{i}\lambda_\alpha/k)$.

The wavefunction on the bond $(\alpha\beta)$ is

$$\varphi_{(\alpha\beta)}(x_{\alpha\beta}) = \exp(\mathrm{i}x_{\alpha\beta}\theta_{\alpha\beta}/l_{\alpha\beta})(\varphi_\alpha f_{\alpha\beta}(x_{\alpha\beta}) + \varphi_\beta \exp(-\mathrm{i}\theta_{\alpha\beta}) f_{\beta\alpha}(x_{\alpha\beta})) \qquad (1)$$

where $\theta_{\alpha\beta}$ is the magnetic flux along the bond $(\alpha\beta)$ (the vector potential is $A_{\alpha\beta} = \theta_{\alpha\beta}/l_{\alpha\beta}$). The two real functions $f_{\alpha\beta}(x)$, $f_{\beta\alpha}(x)$ are the two linearly independent solutions of the

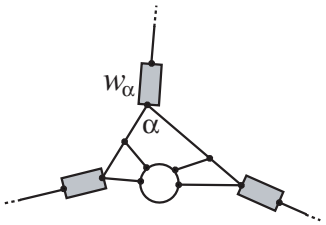

Figure 1. Example of graph. The boxes represent the couplings between the infinite leads and the graph.

Schrödinger equation $\left[E + \mathrm{d}_x^2 - V_{(\alpha\beta)}(x)\right] f(x) = 0$ on the bond satisfying boundary conditions: $f_{\alpha\beta}(0) = 1$, $f_{\alpha\beta}(l_{\alpha\beta}) = 0$, $f_{\beta\alpha}(0) = 0$ and $f_{\beta\alpha}(l_{\alpha\beta}) = 1$. These two functions encode the information about the potential on the bond. For example, in the absence of potential, $V(x) = 0$, we have $f_{\alpha\beta}(x_{\alpha\beta}) = \sin k(l_{\alpha\beta} - x_{\alpha\beta})/\sin k l_{\alpha\beta}$.

The graph is connected to L leads. Each lead is a semi-infinite line plugged at a vertex of the graph, with a coupling parameter $w_\alpha \in \mathbb{R}$ (see figure 1). The introduction of these couplings allows us to go continuously from an isolated graph to a connected one. The precise physical meaning of these parameters is given in [10]. In particular, the transmission amplitude through the box between the graph and the lead is $2w_\alpha/\left(1 + w_\alpha^2\right)$. We introduce the $L \times V$ matrix W:

$$W_{\alpha\beta} = w_\alpha \delta_{\alpha\beta} \tag{2}$$

where α belongs to the set of vertices connected to leads and β to the set of all vertices of the graph. This matrix encodes the information about the way the graph is connected to the external leads.

The scattering matrix Σ is a $L \times L$ matrix describing how a plane wave of energy E entering from a lead is scattered into the other leads by the graph. It is given by

$$\Sigma = -1 + 2W \frac{1}{M + W^{\mathrm{T}} W} W^{\mathrm{T}} \tag{3}$$

where the matrix M is

$$M_{\alpha\beta}(-E) = \frac{\mathrm{i}}{\sqrt{E}} \left(\delta_{\alpha\beta} \left[\lambda_\alpha - \sum_\mu a_{\alpha\mu} \frac{\mathrm{d} f_{\alpha\mu}}{\mathrm{d} x_{\alpha\mu}}(\alpha) \right] + a_{\alpha\beta} \frac{\mathrm{d} f_{\alpha\beta}}{\mathrm{d} x_{\alpha\beta}}(\beta) \exp(\mathrm{i}\theta_{\alpha\beta}) \right). \tag{4}$$

Note that for $E > 0$, this matrix is anti-Hermitian: $M^\dagger = -M$. It can also be related [10] to reflection and transmission coefficients describing the potential on each bond:

$$M_{\alpha\beta}(-E) = \delta_{\alpha\beta} \left(\mathrm{i} \frac{\lambda_\alpha}{\sqrt{E}} + \sum_\mu a_{\alpha\mu} \frac{(1 - r_{\alpha\mu})(1 + r_{\mu\alpha}) + t_{\alpha\mu} t_{\mu\alpha}}{(1 + r_{\alpha\mu})(1 + r_{\mu\alpha}) - t_{\alpha\mu} t_{\mu\alpha}} \right) - a_{\alpha\beta} \frac{2 t_{\alpha\beta}}{(1 + r_{\alpha\beta})(1 + r_{\beta\alpha}) - t_{\alpha\beta} t_{\beta\alpha}}. \tag{5}$$

The expressions (4), (5), together with (3), generalize results known in the absence of the potential [6].

The vertex formulation that we have just recalled is rather efficient mainly because vertex matrices are rather compact. However, as we have noted, it corresponds to a particular choice of vertex scattering which does not describe all allowed relevant physical situations. In the most general situation it is no longer possible to introduce vertex variables and one has to use the arc formulation that will now be briefly described.

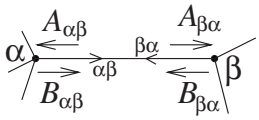

Figure 2. The internal amplitudes associated with the arcs $\alpha\beta$ and $\beta\alpha$.

2.2. Arc formulation

An arc is an oriented bond. On each arc i we introduce an amplitude A_i arriving at the vertex from which i issues and an amplitude B_i departing from it (see figure 2). Equivalently, the wavefunction $\psi_i(x)$ on the bond is matched with $A_i \exp(-\mathrm{i}kx) + B_i \exp(\mathrm{i}kx)$ at the extremity of the arc. It is clear then we have to introduce L such couples of amplitudes, one for each external lead. These external amplitudes are gathered in L column vectors A^{ext} and B^{ext}. By definition the scattering matrix relates these amplitudes: $B^{\mathrm{ext}} = \Sigma A^{\mathrm{ext}}$. On the other hand we must introduce two couples of amplitudes A_i, B_i per bond of the graph, i.e. one couple per arc. We gather these $2B$ amplitudes into the column vectors A^{int} and B^{int}. Finally we group all amplitudes, internal and external, into two $2B + L$ column vectors A and B.

The scattering by the bonds is described by a matrix R coupling reversed internal arcs: $A^{\mathrm{int}} = RB^{\mathrm{int}}$. The matrix element between arcs i and j is given by

$$R_{ij} = r_i \delta_{i,j} + t_{\bar{i}} \delta_{\bar{i},j} \tag{6}$$

where $\bar{i}$ designate the reversed arc. r_i and t_i are the reflection and transmission coefficients describing the scattering of a plane wave by the potential of the bond (i). The scattering at the vertices is described by a matrix Q coupling arcs issuing from the same vertex: $B = QA$. If the basis of arcs is organized as {internal arcs, external arcs}, the matrix Q can be separated into blocks:

$$Q = \left(\begin{array}{c|c} Q^{\mathrm{int}} & \tilde{Q}^{\mathrm{T}} \\ \hline \tilde{Q} & Q^{\mathrm{ext}} \end{array}\right). \tag{7}$$

The scattering matrix reads

$$\Sigma = Q^{\mathrm{ext}} + \tilde{Q}(R^{\dagger} - Q^{\mathrm{int}})^{-1}\tilde{Q}^{\mathrm{T}}. \tag{8}$$

For more details, see [10]. Historically, the arc approach has been followed in many works, such as [30–32] since it is the most natural approach. It has been formalized more systematically in [33] without potential and in [10] in the most general case.

How can we express the wavefunction inside the graph within the arc formulation? In this case, the appropriate basis of solutions of the Schrödinger equation on the bond $\left[E + \mathrm{d}_x^2 - V_{(\alpha\beta)}(x)\right] f(x) = 0$ is no longer the functions $f_{\alpha\beta}(x)$ and $f_{\beta\alpha}(x)$ introduced above, but the couple of stationary scattering states $\phi_{\alpha\beta}(x)$ and $\phi_{\beta\alpha}(x)$ associated with the potential $V_{(\alpha\beta)}(x)$ on the bond $(\alpha\beta)$. If we imagine that the potential $V_{(\alpha\beta)}(x)$ is embedded in $\mathbb{R}$, then the function $\phi_{\alpha\beta}(x)$ is the scattering state incoming on the potential from the vertex α and is matched out of the bond to: $\phi_{\alpha\beta}(x) = \exp(\mathrm{i}kx) + r_{\alpha\beta}\exp(-\mathrm{i}kx)$ for $x < 0$ and $\phi_{\alpha\beta}(x) = t_{\alpha\beta}\exp(\mathrm{i}k(x - l_{\alpha\beta}))$ for $x > l_{\alpha\beta}$ [10].

Then the component of the wavefunction $\varphi(x)$ on the bond $(\alpha\beta)$ reads

$$\varphi_{(\alpha\beta)}(x_{\alpha\beta}) = B_{\alpha\beta}\phi_{\alpha\beta}(x_{\alpha\beta}) + B_{\beta\alpha}\phi_{\beta\alpha}(x_{\alpha\beta}). \tag{9}$$

3. Charge of the graph

This section is devoted to the study of the charge distribution in the graph. Our discussion will focus on the average and correlation of the total charge of the graph. The average charge and the zero frequency charge noise can be related to the graph's scattering matrix. These relations provide an extension of the Feynman–Hellman theorem for open systems in an out-of-equilibrium situation. Then, we present a detailed study of the charge noise at finite frequency, emphasizing the effect of the non-equilibrium regime. For simplicity, we shall work at vanishing temperature.

It is convenient to use the language of 'second-quantization' and introduce the field operator:

$$\hat{\psi}(x,t) = \sum_{\alpha=1}^{L} \int_0^\infty \mathrm{d}E\ \tilde{\psi}_E^{(\alpha)}(x)\hat{a}_\alpha(E)\exp(-\mathrm{i}Et) \tag{10}$$

where $\hat{a}_\alpha(E)$ is the annihilation operator associated with the stationary scattering state $\tilde{\psi}_E^{(\alpha)}(x)$ corresponding to a plane wave of energy E injected from the lead α. Note that $\hat{\psi}(x,0)\big|\tilde{\psi}_E^{(\alpha)}\big\rangle = \tilde{\psi}_E^{(\alpha)}(x)|\,\text{vacuum}\,\rangle$.

Studying the charge distribution for graphs with localized states [11, 13, 34] would require taking into account the contribution of the discrete spectrum in the field operator: $\sum_n \sum_{j=1}^{g_n} \varphi_{n,j}(x)\hat{a}_{n,j}\exp(-\mathrm{i}E_n t)$ (the function $\varphi_{n,j}(x)$ is an eigenstate of energy E_n localized in the graph and thus normalized to unity in the graph, and j denotes a degeneracy label). However, such a situation is not generic but arises from symmetries of the graph. For this reason, we shall not discuss it here.

In a non-equilibrium situation, the quantum statistical average gives: $\big\langle \hat{a}_\alpha^\dagger(E)\hat{a}_\beta(E')\big\rangle = \delta_{\alpha\beta}\delta(E-E')f_\alpha(E)$ where $f_\alpha(E)$ is the Fermi–Dirac distribution function giving the occupation of the scattering states coming from the lead α.

Charge operator. The charge operator is

$$\hat{Q}(t) = \int_{\text{Graph}} \mathrm{d}x\,\hat{\psi}^\dagger(x,t)\hat{\psi}(x,t). \tag{11}$$

We introduce its matrix elements on the shell of energy E:

$$\rho^{(\alpha,\beta)}(E) = \big\langle \tilde{\psi}_E^{(\alpha)}\big|\hat{Q}(t)\big|\tilde{\psi}_E^{(\beta)}\big\rangle. \tag{12}$$

Since the spectrum is continuous, these matrix elements have the dimension of a density of states (DoS). They can be related to the scattering matrix

$$\rho^{(\alpha,\beta)}(E) = -\frac{1}{2\mathrm{i}\pi}\left(\Sigma^\dagger\frac{\mathrm{d}\Sigma}{\mathrm{d}U}\right)_{\alpha\beta} \tag{13}$$

where U is a constant potential added inside the graph only (the variable conjugate to the charge of the graph). Instead of differentiating with respect to some additional background potential U, it is also possible to relate it to the derivative with respect to the energy:

$$\rho^{(\alpha,\beta)}(E) = \int_{\text{Graph}} \mathrm{d}x\,\tilde{\psi}_E^{(\alpha)}(x)^*\tilde{\psi}_E^{(\beta)}(x) = \frac{1}{2\mathrm{i}\pi}\left(\Sigma^\dagger\frac{\mathrm{d}\Sigma}{\mathrm{d}E} + \frac{1}{4E}(\Sigma - \Sigma^\dagger)\right)_{\alpha\beta}. \tag{14}$$

Note that $\sum_\alpha \rho^{(\alpha,\alpha)}(E)$ is the DoS of the graph, i.e. the local DoS integrated inside the graph. These relations are proved in appendix C.

Average charge. The average charge

$$\langle\hat{Q}(t)\rangle = \sum_\alpha \int_0^\infty \mathrm{d}E f_\alpha(E)\int_{\text{Graph}} \mathrm{d}x\big|\tilde{\psi}_E^{(\alpha)}(x)\big|^2 = \sum_\alpha \int_0^\infty \mathrm{d}E f_\alpha(E)\rho^{(\alpha,\alpha)}(E) \tag{15}$$

involves the injectivities $\rho(x,\alpha;E) = \left|\tilde{\psi}_E^{(\alpha)}(x)\right|^2$, which are the contributions to the local density of states (LDoS) coming from the scattering state $\tilde{\psi}_E^{(\alpha)}(x)$. The contribution $\rho^{(\alpha,\alpha)}(E)$ of the scattering state $\tilde{\psi}_E^{(\alpha)}$ to the DoS of the graph is weighted by the occupation Fermi factor in the lead α. This illustrates the necessity of the concept of injectivities, emissivities, etc, in the context of out-of-equilibrium systems [3, 35] (see also [13] for a discussion in the context of graphs).

Charge correlation function. The charge correlation function is defined as

$$S_{QQ}(\omega) = \int_{-\infty}^{+\infty} \mathrm{d}(t-t')(\langle \hat{Q}(t)\hat{Q}(t')\rangle - \langle \hat{Q}(t)\rangle\langle \hat{Q}(t')\rangle)\exp(\mathrm{i}\omega(t-t')). \tag{16}$$

In appendix A, the relation between this unsymmetrized correlator and the other one ($Q(t)$ and $Q(t')$ in reverse order) is clarified. Definition (16) matches with that used in [23] which contains a detailed discussion of the relation between the unsymmetrized correlator and transition rates in a two-level system linearly coupled to the charge operator.

Using the relation $\langle \hat{a}_\alpha^\dagger \hat{a}_\beta \hat{a}_\mu^\dagger \hat{a}_\nu\rangle - \langle \hat{a}_\alpha^\dagger \hat{a}_\beta\rangle\langle \hat{a}_\mu^\dagger \hat{a}_\nu\rangle = \delta_{\alpha\nu}\delta_{\beta\mu} f_\alpha(1-f_\beta)$ we obtain

$$S_{QQ}(\omega) = 2\pi \sum_{\alpha,\beta} \int_0^\infty \mathrm{d}E f_\alpha(E)[1-f_\beta(E+\omega)] \left| \int_{\mathrm{Graph}} \mathrm{d}x\, \tilde{\psi}_E^{(\alpha)}(x)^* \tilde{\psi}_{E+\omega}^{(\beta)}(x) \right|^2. \tag{17}$$

Only the zero-frequency correlations involve the $\rho^{(\alpha,\beta)}(E)$:

$$S_{QQ}(\omega=0) = 2\pi \sum_{\alpha,\beta} \int_0^\infty \mathrm{d}E f_\alpha(E)[1-f_\beta(E)]\rho^{(\alpha,\beta)}(E)\rho^{(\beta,\alpha)}(E). \tag{18}$$

Using equation (14) the zero-frequency noise of the total charge is related to the scattering matrix of the graph.

Charge fluctuations. The charge fluctuations at a given time involve the integral of the full spectrum:

$$q_2 = \langle \hat{Q}(t)^2\rangle - \langle \hat{Q}(t)\rangle^2 = \frac{1}{2\pi}\int \mathrm{d}\omega S_{QQ}(\omega). \tag{19}$$

In terms of the stationary scattering states, we get

$$q_2 = \sum_{\alpha,\beta} \int_0^\infty \mathrm{d}E\, \mathrm{d}E' f_\alpha(E)[1-f_\beta(E')] \left| \int_{\mathrm{Graph}} \mathrm{d}x\, \tilde{\psi}_E^{(\alpha)}(x)^* \tilde{\psi}_{E'}^{(\beta)}(x) \right|^2. \tag{20}$$

3.1. Weakly connected graphs

To go further let us focus on the case of graphs weakly coupled to the leads ($w_\alpha \to 0$). Note that we do not consider charging effect in the following (Coulomb blockade) which is important if the capacitance describing the Coulomb interaction between the leads and the graph is small (see [36] for a review article). A description of such effects would require a different approach. However, in the neighbourhood of the Coulomb peak, a description within the scattering approach can be sufficient to describe transport, like it has been done very recently in [49] to analyse Fano profile measurements in a ring with a dot embedded in one of its arms.

If $w_\alpha \to 0$ the decomposition of the scattering states over the resonances (levels of the isolated graph), derived in appendix B, can be used,

$$\tilde{\psi}_E^{(\alpha)}(x) \simeq \sum_n \frac{1}{\sqrt{\pi}} \frac{\mathrm{i}E_n^{1/4} w_\alpha \varphi_n^*(\alpha)}{E - E_n + \mathrm{i}\Gamma_n} \varphi_n(x). \tag{21}$$

Here $\varphi_n(x)$ denotes the wavefunction of the eigenstate of energy E_n of the isolated graph, normalized to unity in the graph. From this expression we get

$$\rho^{(\alpha,\beta)}(E) \simeq \sum_n \frac{1}{\pi} \frac{\sqrt{\Gamma_{n,\alpha}\Gamma_{n,\beta}}\exp(\mathrm{i}\chi_{\alpha\beta})}{(E-E_n)^2+\Gamma_n^2} \tag{22}$$

where $\Gamma_{n,\alpha} = \sqrt{E_n} w_\alpha^2 |\varphi_n(\alpha)|^2$ is the contribution of the contact α to the resonance width $\Gamma_n = \sum_\alpha \Gamma_{n,\alpha}$. The phase is given by $\exp(\mathrm{i}\chi_{\alpha\beta}) = \varphi_n(\alpha)^* \varphi_n(\beta)/|\varphi_n(\alpha)\varphi_n(\beta)|$.

3.1.1. Average charge. Equation (15) gives

$$\langle \hat{Q}(t)\rangle \simeq \sum_\alpha \int_0^\infty \mathrm{d}E f_\alpha(E) \sum_n \frac{\Gamma_{n,\alpha}/\pi}{(E-E_n)^2+\Gamma_n^2} = \sum_n \sum_\alpha \frac{\Gamma_{n,\alpha}}{\Gamma_n}\left(\frac{1}{\pi}\arctan\frac{V_\alpha - E_n}{\Gamma_n} + \frac{1}{2}\right) \tag{23}$$

where the sum over n runs over the energies of the resonances (energies of the isolated graph). V_α is the potential at contact α. This equation was derived in [37] by tracing out the lead's degrees of freedom. Since the average charge is the sum of contributions of the various levels, we can consider only one level E_n. If the level is below the potentials, $E_n < V_R < V_L$, the occupation of the level is 1. On the other hand, if the level E_n is between the potentials, $V_R < E_n < V_L$, and far enough from them (on the scale Γ_n), it gives a contribution $\Gamma_{n,L}/\Gamma_n$ to the average charge, which simply expresses that only the left scattering state is contributing to the occupation of the resonant level.

3.1.2. Charge noise at finite frequency. Let us now discuss the finite frequency structure of the charge noise for weakly connected graphs. Equation (17) requires evaluating

$$\left|\int_{\mathrm{Graph}} \mathrm{d}x \tilde{\psi}_E^{(\alpha)}(x)^* \tilde{\psi}_{E+\omega}^{(\beta)}(x)\right|^2 \simeq \left|\sum_n \frac{1}{\pi} \frac{\sqrt{E_n} w_\alpha w_\beta \varphi_n(\alpha)\varphi_n^*(\beta)}{(E-E_n-\mathrm{i}\Gamma_n)(E+\omega-E_n+\mathrm{i}\Gamma_n)}\right|^2. \tag{24}$$

Let us keep only the diagonal elements in the double sum. This diagonal approximation is valid in the limit of narrow resonances ($\Gamma_n \ll |E_{n+1}-E_n|$) since the energies E and $E+\omega$ are then compelled to both be in the neighbourhood of the level E_n. Then the correlation appears as a sum of contributions of the different energy levels:

$$S_{QQ}(\omega) \simeq \sum_n S_{QQ}^{(n)}(\omega). \tag{25}$$

The contribution of the level E_n reads

$$S_{QQ}^{(n)}(\omega) = 2\pi \sum_{\alpha,\beta} \int \mathrm{d}E f_\alpha(E)[1-f_\beta(E+\omega)] \frac{\Gamma_{n,\alpha}/\pi}{(E-E_n)^2+\Gamma_n^2} \frac{\Gamma_{n,\beta}/\pi}{(E+\omega-E_n)^2+\Gamma_n^2}. \tag{26}$$

Performing the integrals leads to

$$S_{QQ}^{(n)}(\omega) = \frac{1}{2\pi}\frac{1}{1+\omega^2/4\Gamma_n^2} \sum_{\alpha,\beta} \frac{\Gamma_{n,\alpha}\Gamma_{n,\beta}}{\Gamma_n^3} \theta(\omega+V_\alpha-V_\beta) A(V_\alpha, V_\beta; \omega) \tag{27}$$

where $\theta(\omega)$ is the Heaviside function and

$$\begin{aligned} A(V_\alpha, V_\beta; \omega) = {} & \arctan\left(\frac{V_\alpha - E_n}{\Gamma_n}\right) - \arctan\left(\frac{V_\beta - E_n}{\Gamma_n}\right) \\ & + \arctan\left(\frac{V_\alpha+\omega-E_n}{\Gamma_n}\right) - \arctan\left(\frac{V_\beta-\omega-E_n}{\Gamma_n}\right) \\ & + \frac{\Gamma_n}{\omega} \ln \frac{\left[(V_\alpha+\omega-E_n)^2+\Gamma_n^2\right]\left[(V_\beta-\omega-E_n)^2+\Gamma_n^2\right]}{\left[(V_\alpha-E_n)^2+\Gamma_n^2\right]\left[(V_\beta-E_n)^2+\Gamma_n^2\right]}. \end{aligned} \tag{28}$$

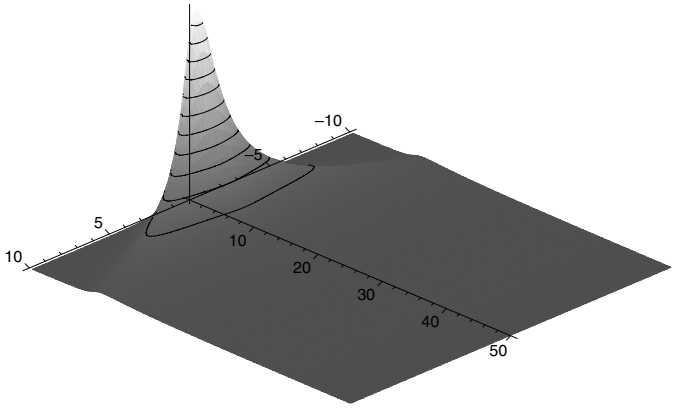

Figure 3. Equilibrium noise in terms of $-10 < \omega/\Gamma_n < 10$ and of the energy of the level $(-E_n)/\Gamma_n$ (this is equivalent to varying the energy or the chemical potential).

For the particular case of a two-terminal geometry the noise reads

$$S_{QQ}^{(n)}(\omega) = \frac{1}{2\pi\Gamma_n^3}\frac{1}{1+\omega^2/4\Gamma_n^2}\big[\Gamma_{n,L}^2\theta(\omega)A(V_L,V_L;\omega)+\Gamma_{n,R}^2\theta(\omega)A(V_R,V_R;\omega) + \Gamma_{n,L}\Gamma_{n,R}\theta(\omega+V)A(V_L,V_R;\omega)+\Gamma_{n,R}\Gamma_{n,L}\theta(\omega-V)A(V_R,V_L;\omega)\big] \quad (29)$$

where $V = V_L - V_R > 0$ is the voltage drop.

- *Equilibrium case:* $V_L = V_R = 0$.

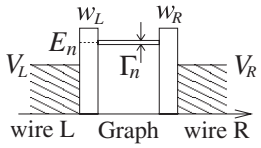

$$S_{QQ}^{(n)}(\omega) = \frac{1}{2\pi\Gamma_n}\frac{\theta(\omega)}{1+\omega^2/4\Gamma_n^2}\left[\arctan\left(\frac{\omega-E_n}{\Gamma_n}\right)+\arctan\left(\frac{\omega+E_n}{\Gamma_n}\right) + \frac{\Gamma_n}{\omega}\ln\frac{\big[(\omega-E_n)^2+\Gamma_n^2\big]\big[(\omega+E_n)^2+\Gamma_n^2\big]}{\big[E_n^2+\Gamma_n^2\big]^2}\right]. \quad (30)$$

We consider the case of narrow resonances where Γ_n is the smallest energy scale, then if the frequency is smaller than $|E_n|$, the contribution is zero, but if ω is sufficiently large to excite an energy level $\omega \gtrsim |E_n|$, we get a contribution:

$$S_{QQ}^{(n)}(\omega) \simeq \frac{1}{2\Gamma_n}\frac{\theta(\omega)}{1+\omega^2/4\Gamma_n^2}\times\begin{cases}0 & \text{if} \quad \omega \lesssim |E_n| \\ 1 & \text{if} \quad \omega \gtrsim |E_n|.\end{cases} \quad (31)$$

Obviously, the transition between the two results is not sharp but occurs on a scale Γ_n. Practically all the noise power is concentrated at low frequencies as shown in figure 3.

Note that this contribution is independent of the fact that the level is occupied ($E_n < 0$) or empty ($E_n > 0$) since it is an even function of E_n. At $V_L = V_R$, the low-frequency charge noise can be understood using a classical stochastic model describing the relaxation process of an electron (or a hole) with lifetime $1/2\Gamma_n$.

- *Non-equilibrium regime:* $V_L \neq V_R$.

Zero-frequency limit. Then only the term with $A(V_L, V_R; 0)$ contributes

$$S_{QQ}^{(n)}(\omega = 0) \simeq \frac{1}{\pi}\frac{\Gamma_{n,R}\Gamma_{n,L}}{\Gamma_n^3}\left\{\arctan\left(\frac{V_L - E_n}{\Gamma_n}\right) + \arctan\left(\frac{E_n - V_R}{\Gamma_n}\right) + \frac{\Gamma_n(V_L - E_n)}{(V_L - E_n)^2 + \Gamma_n^2} + \frac{\Gamma_n(E_n - V_R)}{(E_n - V_R)^2 + \Gamma_n^2}\right\}. \tag{32}$$

Each energy level brings a contribution only if it is between the potentials ($V_R < E_n < V_L$) and far enough from them (on the scale Γ_n). In this case, the zero-frequency charge noise is given by

$$S_{QQ}^{(n)}(\omega = 0) \simeq \frac{\Gamma_{n,R}\Gamma_{n,L}}{\Gamma_n^3}. \tag{33}$$

We recognize the factor $\Gamma_{n,R}\Gamma_{n,L}$ characteristic of partition noise: if one of the couplings vanishes ($\Gamma_{n,R} = 0$ or $\Gamma_{n,L} = 0$) the occupation of the level is either 0 or 1 and does not fluctuate. These fluctuations are a signature of the non-equilibrium regime of the mesoscopic circuit. The charge fluctuations at fixed time can be obtained by integrating the noise spectrum (19). Using the approximate expression (21) in (20) we obtain

$$q_2 \simeq \sum_n \sum_{\alpha,\beta} \frac{\Gamma_{n,\alpha}\Gamma_{n,\beta}}{\Gamma_n^2}\left(\frac{1}{\pi}\arctan\frac{V_\alpha - E_n}{\Gamma_n} + \frac{1}{2}\right)\left(\frac{1}{\pi}\arctan\frac{E_n - V_\beta}{\Gamma_n} + \frac{1}{2}\right). \tag{34}$$

In the two-lead case, only the levels between the two potentials make a contribution

$$q_2 \simeq \frac{\Gamma_{n,L}\Gamma_{n,R}}{\Gamma_n^2}. \tag{35}$$

Note that this result cannot be simply inferred from the current shot noise. Near a resonance, the transmission probability through the graph is $T(E) \simeq 4\Gamma_{n,L}\Gamma_{n,R}\big/\left[(E - E_n)^2 + \Gamma_n^2\right]$. The average current in the lead is given by the Landauer formula $\langle I\rangle = (1/2\pi)\int_{V_R}^{V_L} \mathrm{d}E T(E)$ whereas the current and the shot noise is given by $S_{II}(\omega = 0) = (1/2\pi)\int_{V_R}^{V_L} \mathrm{d}E T(E)(1 - T(E))$ [1, 2, 38]. If only one level E_n lies between the two potentials, we obtain in this nonlinear regime [39]: $\langle I\rangle \simeq 2\Gamma_{n,R}\Gamma_{n,L}/\Gamma_n$ and $S_{II}(\omega = 0) \simeq 2\big(\Gamma_{n,R}\Gamma_{n,L}\big/\Gamma_n^3\big)\big(\Gamma_{n,R}^2 + \Gamma_{n,L}^2\big)$.

Finite-frequency noise. Let us choose the origin of the energies in such a way that: $V_R = 0, V_L = V > 0$. Four energy scales must be considered: E_n, Γ_n, V and ω. Several regimes can be observed according to the frequency. To help the discussion we neglect the smallest scale, supposed to be Γ_n, as we did above.

(i) Let us first discuss the case of a fully occupied level: $E_n < V_R = 0$.

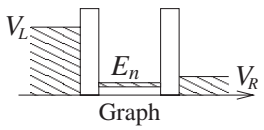

Graph

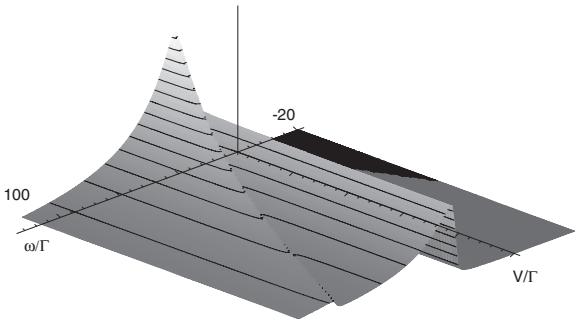

Figure 4. Non-equilibrium noise in terms of $-20 < \omega/\Gamma_n < 100$ and of the voltage drop V/Γ_n for a fully populated level ($V_R = E_n + 50\Gamma_n$).

At small frequencies, correlations are roughly zero. When ω reaches $V_R - E_n$, contributions from the second and third terms appear, while all terms contribute for ω larger than $V_L - E_n$. To summarize these three regimes:

$$S^{(n)}_{QQ}(\omega) \simeq \frac{1}{2\Gamma_n}\frac{1}{1+\omega^2/4\Gamma_n^2} \times \begin{cases} 0 & \text{if} \quad \omega \lesssim V_R - E_n \\ \Gamma_{n,R}/\Gamma_n & \text{if} \quad V_R - E_n \lesssim \omega \lesssim V_L - E_n \\ 1 & \text{if} \quad V_L - E_n \lesssim \omega \end{cases} \tag{36}$$

where we have factorized the equilibrium result.

In the second regime $V_R - E_n \lesssim \omega \lesssim V_L - E_n$, the energy ω is sufficient to excite the state originating from the right reservoir but not from the left reservoir. This is the origin of the ratio $\Gamma_{n,R}/\Gamma_n$. In the third regime, both reservoirs contribute to the noise. At fixed non-zero bias voltage, this leads to a double peak structure in terms of the ω which corresponds to the threshold for creating electron–hole pairs involving the left and right leads (see figure 4). At small V these two peaks tend to merge into a single more pronounced one. At large V the second peak occurs at a larger frequency and is less pronounced because of the Lorentzian factor.

(ii) Let us now discuss the case of an empty level: $E_n > V_L$.

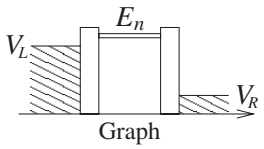

Graph

The physical picture can be obtained using a hole picture. Three different regimes can also be distinguished:

$$S^{(n)}_{QQ}(\omega) \simeq \frac{1}{2\Gamma_n}\frac{1}{1+\omega^2/4\Gamma_n^2} \times \begin{cases} 0 & \text{if} \quad \omega \lesssim E_n - V_L \\ \Gamma_{n,L}/\Gamma_n & \text{if} \quad E_n - V_L \lesssim \omega \lesssim E_n - V_R \\ 1 & \text{if} \quad E_n - V_R \lesssim \omega. \end{cases} \tag{37}$$

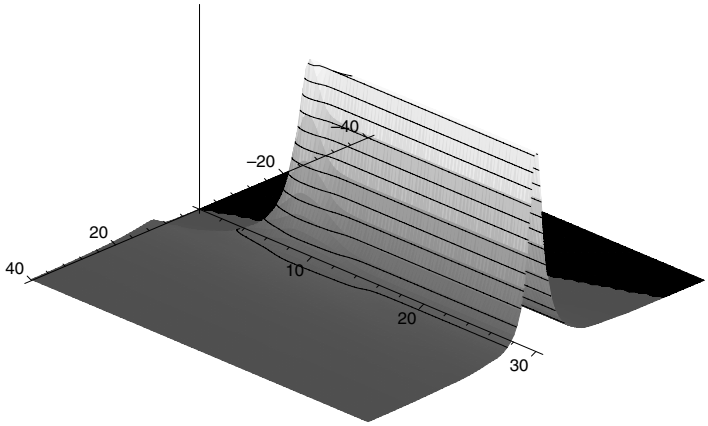

Figure 5. Non-equilibrium noise in terms of $-40 < \omega/\Gamma_n < 40$ and of V/Γ_n. The right lead chemical potential is fixed to $-10\Gamma_n$. Case (iii) corresponds to $V > 10\Gamma_n$ and exhibits an important low-frequency noise whereas $V < 10\Gamma_n$ corresponds to case (ii).

(iii) Finally we consider the case of a level between the two potentials $V_R < E_n < V_L$.

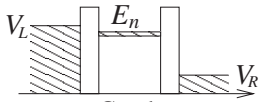

Graph

Considering the case where the level is closer to V_L than to V_R, we obtain

$$S_{QQ}^{(n)}(\omega) \simeq \frac{1}{2\Gamma_n}\frac{1}{1+\omega^2/4\Gamma_n^2} \times \begin{cases} 0 & \text{if} \quad \omega \lesssim -E_n + V_R \\ \Gamma_{n,L}\Gamma_{n,R}/\Gamma_n^2 & \text{if} \quad -E_n + V_R \lesssim \omega \lesssim -V_L + E_n \\ 2\Gamma_{n,L}\Gamma_{n,R}/\Gamma_n^2 & \text{if} \quad -V_L + E_n \lesssim \omega \lesssim V_L - E_n \\ \left(2\Gamma_{n,L}\Gamma_{n,R} + \Gamma_{n,L}^2\right)/\Gamma_n^2 & \text{if} \quad V_L - E_n \lesssim \omega \lesssim E_n - V_R \\ 1 & \text{if} \quad E_n - V_R \lesssim \omega. \end{cases} \tag{38}$$

The fluctuation spectrum is symmetric in the interval centred around $\omega = 0$ with width of order V. The main contribution to the noise appears at low frequency as can be seen from figure 5. The multiple plot (figure 6) shows how the low-frequency peak develops when V_L crosses the energy level.

Interestingly, correlations are proportional to the partition factor $\Gamma_{n,R}\Gamma_{n,L}$ only for small frequencies $|\omega| \ll V$ (or large timescales $t \gg 1/V$). For large frequencies $|\omega| \gg V$, the partition factor does not appear. The high-frequency part of the charge fluctuation spectrum is insensitive to the fact that the system is out of equilibrium. In this limit, the equilibrium result (31) is recovered.

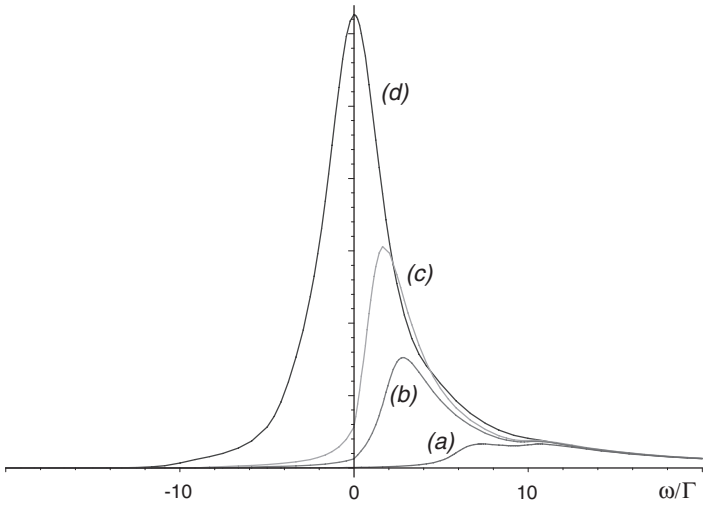

Figure 6. Multiple plots of non-equilibrium charge noise in terms of $-20 < \omega/\Gamma_n < 20$ for different values of V/Γ_n. The right lead chemical potential is fixed as in figure 5. (*a*) $V/\Gamma_n = 4$, (*b*) $V/\Gamma_n = 8$, (*c*) $V/\Gamma_n = 9$ and (*d*) $V/\Gamma_n = 14$.

4. Currents inside the graph

A possible way to probe a mesoscopic device is to attach some leads to it, through which some currents are injected. Some information can be extracted from transport or noise properties: average values and correlations of currents in the *external* leads. All these properties can be related to the scattering matrix (see [39] for a review). If one is now interested in local information on the system, like the measurement of a persistent current, a natural way would be to introduce some local probe. However, as we have recalled in the introduction, local information can also be extracted from scattering properties. Here, we investigate the currents in the *internal* wires, and show the relation to the scattering properties. The starting point, exposed in the introduction, is the relation between the current in a wire and the derivative of the scattering matrix with respect to its conjugate variable, the flux in the wire. This idea comes from [17] and has been elaborated further in [29] to include derivation of correlations of the current density. Here, we focus on the case of graphs in the context of which we will generalize these previous results to the non-equilibrium situation.

4.1. Current in a closed graph

First we derive an expression for the current density in a closed graph. It is convenient to introduce the spectral determinant of the Schrödinger operator

$$S(\gamma) = \det(-\Delta + V(x) + \gamma) = \prod_n (E_n + \gamma) \tag{39}$$

where γ is a spectral parameter. The set of E_n is the spectrum of the Schrödinger operator on the graph. It was shown in [40–43] that the spectral determinant, which is the determinant of an unbounded operator, can be related to the determinant of a finite-size matrix. In the vertex approach, formula (100) involves a $V \times V$ matrix, whereas in the arc language the spectral determinant involves a $2B \times 2B$ matrix: $S(-E) \propto \det(1 - QR)$ [41, 43]. Note that for a closed graph, the vertex scattering matrix Q has the same dimension as the bond

scattering matrix. We introduce the current density $j(E)$ associated with the states in the interval $[E, E + \mathrm{d}E[$. The current density in the arc a is

$$j_a(E) = -\sum_n \delta(E - E_n)\frac{\partial E_n}{\partial \theta_a} = \frac{1}{\pi}\mathrm{Im}\,\frac{\partial}{\partial \theta_a}\ln S(-E + \mathrm{i}0^+) \tag{40}$$

where θ_a is the magnetic flux along this arc.

Example. Consider a closed ring of perimeter l threaded by a flux θ. Its spectral determinant is $S(\gamma) = \mathrm{ch}(\sqrt{\gamma}l) - \cos(\theta)$ [41]. We write: $\gamma = -k^2 + \mathrm{i}0^+$, then $\mathrm{ch}(\sqrt{\gamma}l) = \cos(kl) + \mathrm{i}0^+\sin(kl)$ and we get for the current density in the ring:

$$j(E) = -\sin\theta\,\mathrm{sign}(\sin kl)\delta(\cos kl - \cos\theta) = \sum_n \delta(E - E_n)I_n \tag{41}$$

with $I_n = -\partial_\theta E_n$ where $E_n = (2n\pi - \theta)^2/l^2$.

4.2. Current in open graphs

Now we consider a graph connected to infinite leads.

The current operator is

$$\hat{J}(x,t) = \frac{1}{\mathrm{i}}[\hat{\psi}^\dagger(x,t)\mathrm{D}_x\hat{\psi}(x,t) - \mathrm{D}_x^*\hat{\psi}^\dagger(x,t)\hat{\psi}(x,t)] \tag{42}$$

where $\mathrm{D}_x = \mathrm{d}_x - \mathrm{i}A(x)$ is the covariant derivative.

We introduce the current matrix elements

$$j_{\mu\nu}^{(\alpha,\beta)}(E) = \left\langle \tilde{\psi}_E^{(\alpha)} \middle| \hat{J}(x,t) \middle| \tilde{\psi}_E^{(\beta)} \right\rangle \qquad \text{for} \quad x \in \mu\nu \tag{43}$$

which can be shown to be independent of the coordinate x along the arc (only if the two states have the same energy). This matrix element can then be computed at the vertex μ ($x = 0$):

$$j_{\mu\nu}^{(\alpha,\beta)}(E) = \frac{1}{\mathrm{i}}\left(\tilde{\psi}_\mu^{(\alpha)*}\mathrm{D}_x\tilde{\psi}_{(\mu\nu)}^{(\beta)}(\mu) - \mathrm{D}_x^*\tilde{\psi}_{(\mu\nu)}^{(\alpha)*}(\mu)\tilde{\psi}_\mu^{(\beta)}\right). \tag{44}$$

The quantum and statistical average of the current operator in the arc $\mu\nu$ gives

$$J_{\mu\nu} = \langle \hat{J}(x \in \mu\nu, t)\rangle = \sum_\alpha \int \mathrm{d}E f_\alpha(E) j_{\mu\nu}^{(\alpha,\alpha)}(E). \tag{45}$$

The correlations (unsymmetrized in time or frequency) between the currents in the arcs $\mu\nu$ and $\mu'\nu'$ are defined as

$$S_{J_{\mu\nu}J_{\mu'\nu'}}(\omega) = \int_{-\infty}^{+\infty} \mathrm{d}(t - t')(\langle \hat{J}(x,t)\hat{J}(x',t')\rangle - \langle \hat{J}(x,t)\rangle\langle \hat{J}(x',t')\rangle)\exp(\mathrm{i}\omega(t - t')) \tag{46}$$

for $x \in \mu\nu$ and $x' \in \mu'\nu'$. They can be rewritten at zero frequency as

$$S_{J_{\mu\nu}J_{\mu'\nu'}}(\omega = 0) = 2\pi\sum_{\alpha,\beta}\int \mathrm{d}E\, f_\alpha(E)[1 - f_\beta(E)]j_{\mu\nu}^{(\alpha,\beta)}(E)j_{\mu'\nu'}^{(\beta,\alpha)}(E). \tag{47}$$

4.2.1. Vertex formulation. Now we look for a relation between the current density and the scattering matrix. We start from the expression of the scattering state in the arc $\mu\nu$:

$$\psi_{(\mu\nu)}(x) = \exp(\mathrm{i}\theta_{\mu\nu}x/l_{\mu\nu})(\psi_\mu f_{\mu\nu}(x) + \psi_\nu\exp(-\mathrm{i}\theta_{\mu\nu})f_{\nu\mu}(x)). \tag{48}$$

Then

$$j_{\mu\nu}^{(\alpha,\beta)} = \frac{1}{\mathrm{i}}\left(-\tilde{\psi}_\mu^{(\alpha)*}\frac{\mathrm{d}f_{\mu\nu}}{\mathrm{d}x_{\mu\nu}}(\nu)\exp(-\mathrm{i}\theta_{\mu\nu})\tilde{\psi}_\nu^{(\beta)} + \tilde{\psi}_\nu^{(\alpha)*}\frac{\mathrm{d}f_{\nu\mu}}{\mathrm{d}x_{\nu\mu}}(\mu)\exp(\mathrm{i}\theta_{\mu\nu})\tilde{\psi}_\mu^{(\beta)}\right) \tag{49}$$

where we have used the fact that the Wronskian of $f_{\mu\nu}(x)$ and $f_{\nu\mu}(x)$ reads: $(\mathrm{d}f_{\nu\mu}/\mathrm{d}x_{\mu\nu})(\mu) = -(\mathrm{d}f_{\mu\nu}/\mathrm{d}x_{\mu\nu})(\nu)$. From the definition of the matrix M, we see that

$$j_{\mu\nu}^{(\alpha,\beta)} = -\frac{k}{\mathrm{i}}\left(\tilde{\psi}_{\mu}^{(\alpha)*}\frac{\mathrm{d}M_{\mu\nu}}{\mathrm{d}\theta_{\mu\nu}}\tilde{\psi}_{\nu}^{(\beta)} + \tilde{\psi}_{\nu}^{(\alpha)*}\frac{\mathrm{d}M_{\nu\mu}}{\mathrm{d}\theta_{\mu\nu}}\tilde{\psi}_{\mu}^{(\beta)}\right). \tag{50}$$

Only the two elements $M_{\mu\nu}$ and $M_{\nu\mu}$ depend on the flux $\theta_{\mu\nu}$, then

$$j_{\mu\nu}^{(\alpha,\beta)} = -\frac{k}{\mathrm{i}}\left(\tilde{\Psi}^{\dagger}\frac{\mathrm{d}M}{\mathrm{d}\theta_{\mu\nu}}\tilde{\Psi}\right)_{\alpha\beta} \tag{51}$$

where $\tilde{\Psi}$ is the $V \times L$-matrix that gathers the values of the L stationary states at the V vertices: $\tilde{\Psi}_{\mu\alpha} \equiv \tilde{\psi}_{\mu}^{(\alpha)}$. This matrix is [10, 13]

$$\tilde{\Psi} = \frac{1}{\sqrt{\pi k}}\frac{1}{M + W^{\mathrm{T}}W}W^{\mathrm{T}}. \tag{52}$$

We can rewrite the current density in terms of matrices M and W:

$$j_{\mu\nu}^{(\alpha,\beta)} = -\frac{1}{\mathrm{i}\pi}\left(W\frac{1}{-M + W^{\mathrm{T}}W}\frac{\mathrm{d}M}{\mathrm{d}\theta_{\mu\nu}}\frac{1}{M + W^{\mathrm{T}}W}W^{\mathrm{T}}\right)_{\alpha\beta}. \tag{53}$$

Our aim is now to find the relation of this expression with the scattering matrix. We use the relation $(\mathrm{d}/\mathrm{d}\eta)A(\eta)^{-1} = -A(\eta)^{-1}(\mathrm{d}A(\eta)/\mathrm{d}\eta)A(\eta)^{-1}$ that gives the derivative of the inverse of a square matrix $A(\eta)$ depending on a parameter η. In expression (3) only M depends on the fluxes, it follows that

$$\frac{\mathrm{d}\Sigma}{\mathrm{d}\theta_{\mu\nu}} = -2W\frac{1}{M + W^{\mathrm{T}}W}\frac{\mathrm{d}M}{\mathrm{d}\theta_{\mu\nu}}\frac{1}{M + W^{\mathrm{T}}W}W^{\mathrm{T}}. \tag{54}$$

If we multiply this expression by $\Sigma^{\dagger}$ from the left, it replaces the M in the left fraction by $-M$. We conclude that the off-diagonal elements of the current density read

$$j_{\mu\nu}^{(\alpha,\beta)}(E) = \frac{1}{2\mathrm{i}\pi}\left(\Sigma^{\dagger}\frac{\mathrm{d}\Sigma}{\mathrm{d}\theta_{\mu\nu}}\right)_{\alpha\beta}. \tag{55}$$

Note that this result is reminiscent of the one obtained by Taniguchi in [29] who derived some relation between the scattering matrix and the 'current density', i.e. the diagonal elements ($\alpha = \beta$) of (55).

4.2.2. Arc formulation. Let us now reformulate the previous demonstration in the arc language which allows us to consider the most general case.

As explained in the introduction, the wavefunction on the bond $(\mu\nu)$ can be expressed as

$$\psi_{(\mu\nu)}(x_{\mu\nu}) = B_{\mu\nu}\phi_{\mu\nu}(x_{\mu\nu}) + B_{\nu\mu}\phi_{\nu\mu}(x_{\mu\nu}) \tag{56}$$

where $\phi_{\mu\nu}(x_{\mu\nu})$ and $\phi_{\nu\mu}(x_{\mu\nu})$ are the left and right stationary scattering states for the bond potential $V_{(\mu\nu)}(x_{\mu\nu})$. Using the expressions of these functions at the extremities of the bond given in the introduction, we get the derivative of the wavefunction at the vertex μ:

$$\mathrm{D}_x\psi_{(\mu\nu)}(\mu) = \mathrm{i}k[B_{\mu\nu}(1 - r_{\mu\nu}) - B_{\nu\mu}t_{\nu\mu}]. \tag{57}$$

We call $\tilde{B}_{\mu\nu}^{(\alpha)}$ the internal amplitude corresponding to the stationary scattering state $\tilde{\psi}_{E}^{(\alpha)}(x)$. These amplitudes are obtained by solving the equations $B = QA$ and $A^{\mathrm{int}} = RB^{\mathrm{int}}$ with external amplitudes A^{ext} describing the injection of a plane wave on the lead arriving at vertex α: its components are $\tilde{A}_i^{(\alpha)\mathrm{ext}} = \sqrt{1/4\pi k}\delta_{i,\mathrm{arc}\,\alpha}$ where 'arc α' designates the arc related to the lead issuing from α. Then the amplitude

$$\tilde{B}_{\mu\nu}^{(\alpha)} = \frac{1}{\sqrt{4\pi k}}[(1 - Q^{\mathrm{int}}R)^{-1}\tilde{Q}^{\mathrm{T}}]_{\mu\nu,\mathrm{arc}\,\alpha} \tag{58}$$

is related to the matrix element between the internal arc $\mu\nu$ and the external arc 'arc α'.

After a little bit of algebra, we get for the current density on the arc $\mu\nu$:

$$j_{\mu\nu}^{(\alpha,\beta)} = 2k\big[\tilde{B}_{\mu\nu}^{(\alpha)*}|t_{\mu\nu}|^2\tilde{B}_{\mu\nu}^{(\beta)} + \tilde{B}_{\mu\nu}^{(\alpha)*}t_{\mu\nu}^* r_{\nu\mu}\tilde{B}_{\nu\mu}^{(\beta)} - \tilde{B}_{\nu\mu}^{(\alpha)*}t_{\nu\mu}^* r_{\mu\nu}\tilde{B}_{\mu\nu}^{(\beta)} - \tilde{B}_{\nu\mu}^{(\alpha)*}|t_{\nu\mu}|^2\tilde{B}_{\nu\mu}^{(\beta)}\big]. \tag{59}$$

We have used $t_{\mu\nu}^* r_{\nu\mu} = -r_{\mu\nu}^* t_{\nu\mu}$ coming from the unitarity of R. In the bond scattering matrix R, only the transmissions depend on the magnetic fluxes: $t_{\mu\nu} \propto \exp(\mathrm{i}\theta_{\mu\nu})$. It follows that, in the matrix $(\mathrm{d}R^\dagger/\mathrm{d}\theta_{\mu\nu})R$, only the 2×2 block related to the arcs $\mu\nu$ and $\nu\mu$ is different from zero. It is given by

$$\mathrm{i}\begin{pmatrix} -|t_{\mu\nu}|^2 & -t_{\mu\nu}^* r_{\nu\mu} \\ t_{\nu\mu}^* r_{\mu\nu} & |t_{\nu\mu}|^2 \end{pmatrix}. \tag{60}$$

Then it is straightforward to see that

$$j_{\mu\nu}^{(\alpha,\beta)} = -2\mathrm{i}k\sum_{i,j}\tilde{B}_i^{(\alpha)*}\left(\frac{\mathrm{d}R^\dagger}{\mathrm{d}\theta_{\mu\nu}}R\right)_{i,j}\tilde{B}_j^{(\beta)} \tag{61}$$

where the sum over i, j runs over the $2B$ internal arcs. Using expression (58) for the amplitudes, we obtain

$$j_{\mu\nu}^{(\alpha,\beta)} = -\frac{1}{2\mathrm{i}\pi}\left(\tilde{Q}^*(1-R^\dagger Q^{\mathrm{int}\,\dagger})^{-1}\frac{\mathrm{d}R^\dagger}{\mathrm{d}\theta_{\mu\nu}}R(1-Q^{\mathrm{int}}R)^{-1}\tilde{Q}^{\mathrm{T}}\right)_{\alpha,\beta} \tag{62}$$

$$= -\frac{1}{2\mathrm{i}\pi}\left(\Sigma^\dagger\tilde{Q}(R^\dagger - Q^{\mathrm{int}})^{-1}\frac{\mathrm{d}R^\dagger}{\mathrm{d}\theta_{\mu\nu}}(R^\dagger - Q^{\mathrm{int}})^{-1}\tilde{Q}^{\mathrm{T}}\right)_{\alpha,\beta} \tag{63}$$

$$= \frac{1}{2\mathrm{i}\pi}\left(\Sigma^\dagger\tilde{Q}\frac{\mathrm{d}}{\mathrm{d}\theta_{\mu\nu}}(R^\dagger - Q^{\mathrm{int}})^{-1}\tilde{Q}^{\mathrm{T}}\right)_{\alpha,\beta} = \frac{1}{2\mathrm{i}\pi}\left(\Sigma^\dagger\frac{\mathrm{d}\Sigma}{\mathrm{d}\theta_{\mu\nu}}\right)_{\alpha,\beta}. \tag{64}$$

We have recovered the formula (55) within the arc language[7]. This demonstrates that equation (55) applies to the most general situation, as expected.

4.2.3. Average current and current correlations in terms of the scattering matrix. The average current can be written, as could have been guessed from the general discussion of the introduction:

$$J_{\mu\nu} = \sum_\alpha\int \mathrm{d}E f_\alpha(E)\frac{1}{2\mathrm{i}\pi}\left(\Sigma^\dagger\frac{\mathrm{d}\Sigma}{\mathrm{d}\theta_{\mu\nu}}\right)_{\alpha\alpha}. \tag{65}$$

The correlations of currents at zero frequency are rewritten in the terms of scattering matrix:

$$S_{J_{\mu\nu}J_{\mu'\nu'}}(\omega=0) = -\frac{1}{2\pi}\sum_{\alpha,\beta}\int \mathrm{d}E\, f_\alpha[1-f_\beta]\left(\Sigma^\dagger\frac{\mathrm{d}\Sigma}{\mathrm{d}\theta_{\mu\nu}}\right)_{\alpha\beta}\left(\Sigma^\dagger\frac{\mathrm{d}\Sigma}{\mathrm{d}\theta_{\mu'\nu'}}\right)_{\beta\alpha}. \tag{66}$$

If $\mu\nu = \mu'\nu'$ this gives the noise of the persistent current. At equilibrium, all potentials are equal, $f_\alpha(E) = f(E)\ \forall\alpha$, and we recover an expression reminiscent of the one given in [29]:

$$S_{J_{\mu\nu}J_{\mu'\nu'}}(\omega=0) = \frac{1}{2\pi}\int \mathrm{d}E f(E)[1-f(E)]\,\mathrm{Tr}\left\{\frac{\mathrm{d}\Sigma}{\mathrm{d}\theta_{\mu\nu}}\frac{\mathrm{d}\Sigma^\dagger}{\mathrm{d}\theta_{\mu'\nu'}}\right\}. \tag{67}$$

In his work, Taniguchi identifies the contribution $((\mathrm{d}\Sigma/\mathrm{d}\theta_{\mu\nu})(\mathrm{d}\Sigma^\dagger/\mathrm{d}\theta_{\mu'\nu'}))_{\alpha\alpha}$ of a given scattering state to this trace. However we see that it is not sufficient to go back to the expression (66) describing the non-equilibrium situation.

[7] We have used the relation $\Sigma^\dagger\tilde{Q}(R^\dagger - Q^{\mathrm{int}})^{-1} = \tilde{Q}^*(1-R^\dagger Q^{\mathrm{int}\,\dagger})^{-1}$, coming from the unitarity of the scattering matrices [13].

4.3. Gauge invariance

Since many formulae involve the fluxes along the wires, it is important to discuss how a gauge transformation would affect them and to check that all the measurable quantities are indeed gauge invariant. A gauge transformation changes the vector potential according to $A(x) \to A(x) + \partial_x \chi(x)$, where $\chi(x)$ is a scalar function. The magnetic flux $\theta_{\mu\nu}$ along the arc $\mu\nu$ is then modified according to

$$\theta_{\mu\nu} \quad \longrightarrow \quad \theta'_{\mu\nu} = \theta_{\mu\nu} + \chi_\mu - \chi_\nu \tag{68}$$

where $\chi_\mu \equiv \chi(\mu)$ is the value taken by the function at the vertex μ. In the vertex approach, we immediatly see from its definition that the matrix M is changed as

$$M_{\mu\nu} \quad \longrightarrow \quad M'_{\mu\nu} = M_{\mu\nu} \exp(\mathrm{i}\chi_\mu - \mathrm{i}\chi_\nu). \tag{69}$$

We can write $M' = \mathcal{U} M \mathcal{U}^\dagger$ where the diagonal unitary matrix reads: $\mathcal{U}_{\alpha\beta} = \delta_{\alpha\beta} \exp(\mathrm{i}\chi_\alpha)$. Since $W^{\mathrm{T}}W$ is also diagonal it is clear that $(\pm M' + W^{\mathrm{T}}W)^{-1} = \mathcal{U}(\pm M + W^{\mathrm{T}}W)^{-1}\mathcal{U}^\dagger$. The scattering matrix changes in the same way:

$$\Sigma_{\alpha\beta} \quad \longrightarrow \quad \Sigma'_{\alpha\beta} = \Sigma_{\alpha\beta} \exp(\mathrm{i}\chi_\alpha - \mathrm{i}\chi_\beta). \tag{70}$$

From (53) or (55) we see that the matrix elements of the current operator pick up a phase through a gauge transformation

$$j_{\mu\nu}^{(\alpha,\beta)} \quad \longrightarrow \quad j_{\mu\nu}^{(\alpha,\beta)} \exp(\mathrm{i}\chi_\alpha - \mathrm{i}\chi_\beta). \tag{71}$$

Nevertheless, the average current (45) and the correlations (47) are gauge invariant, as they should be.

4.4. Weakly connected graphs

As we did for the charge distribution, it is interesting to consider the case of graphs weakly connected to the leads ($w_\alpha \to 0$) for which interesting results can be derived. The starting point is again the expression (21) of the scattering state near a resonance (when E is close to an eigenenergy of the isolated graph). Using this relation, the current density matrix element can be expressed as

$$j_{\mu\nu}^{(\alpha,\beta)}(E, E') = \left\langle \tilde{\psi}_E^{(\alpha)} \middle| \hat{J}(x \in \mu\nu, t = 0) \middle| \tilde{\psi}_{E'}^{(\beta)} \right\rangle \tag{72}$$

$$\underset{E, E' \sim E_n}{\simeq} \frac{\sqrt{E_n}}{\pi} \frac{w_\alpha \varphi_n(\alpha)}{E - E_n - \mathrm{i}\Gamma_n} \frac{w_\beta \varphi_n^*(\beta)}{E' - E_n + \mathrm{i}\Gamma_n} I_{\mu\nu}^n \tag{73}$$

where $I_{\mu\nu}^n$ is the current in the arc $\mu\nu$ associated with the eigenstate $\varphi_n(x)$ of the isolated graph:

$$I_{\mu\nu}^n = -\mathrm{i}\varphi_n^*(x) \mathrm{D}_x \varphi_n(x) + \mathrm{c.c.} \qquad \text{for} \quad x \in \mu\nu. \tag{74}$$

Note that in principle the current matrix element (72) between scattering states of different energies depends on the coordinate x, however in the weak coupling limit, since the two scattering states are proportional to the same eigenstate $\varphi_n(x)$, the matrix element becomes x independent.

Equation (72) shows that the calculation of the average current is very similar to the calculation of the charge (23):

$$J_{\mu\nu} \simeq \sum_\alpha \int_0^\infty \mathrm{d}E f_\alpha \sum_n \frac{I_{\mu\nu}^n \Gamma_{n,\alpha}/\pi}{(E - E_n)^2 + \Gamma_n^2} = \sum_n I_{\mu\nu}^n \sum_\alpha \frac{\Gamma_{n,\alpha}}{\Gamma_n} \left(\frac{1}{\pi} \arctan \frac{V_\alpha - E_n}{\Gamma_n} + \frac{1}{2} \right). \tag{75}$$

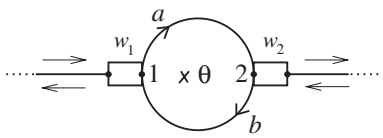

Figure 7. A ring with two arms of lengths l_a and l_b, threaded by a flux θ and coupled with two leads, with coupling parameters $w_{1,2}$. The boxes represent the tunable couplings, with transmission amplitudes $2w_{1,2}/(1+w_{1,2}^2)$ (see [10]).

The contribution of the resonant level can be written

$$J_{\mu\nu}^{(n)} \simeq I_{\mu\nu}^{n} \langle \hat{Q}(t) \rangle^{(n)} \tag{76}$$

where $\langle \cdots \rangle^{(n)}$ designates the contribution of the resonant level n.

Similarly we obtain for the correlations:

$$S_{J_{\mu\nu}J_{\mu'\nu'}}^{(n)}(\omega) \simeq I_{\mu\nu}^{n} I_{\mu'\nu'}^{n} \, S_{QQ}^{(n)}(\omega). \tag{77}$$

For example, for a situation with two contacts with a potential drop V and only one resonant level contributing we get

$$J_{\mu\nu} \simeq I_{\mu\nu}^{n} \frac{\Gamma_{n,L}}{\Gamma_n} \tag{78}$$

and

$$S_{J_{\mu\nu}J_{\mu'\nu'}}(0) \simeq I_{\mu\nu}^{n} I_{\mu'\nu'}^{n} \frac{\Gamma_{n,L}\Gamma_{n,R}}{\Gamma_n^3}. \tag{79}$$

4.5. Example

Let us focus on the simple example of a ring with two leads (see figure 7).

The scattering matrix of the ring reads

$$\Sigma = -1 + \frac{2}{\tilde{S}} \begin{pmatrix} \mathrm{i}w_1^2 \sin kl + w_1^2 w_2^2 s_a s_b & \mathrm{i}w_1 w_2 (s_b \exp(-\mathrm{i}\theta_a) + s_a \exp(\mathrm{i}\theta_b)) \\ \mathrm{i}w_2 w_1 (s_b \exp(\mathrm{i}\theta_a) + s_a \exp(-\mathrm{i}\theta_b)) & \mathrm{i}w_2^2 \sin kl + w_1^2 w_2^2 s_a s_b \end{pmatrix} \tag{80}$$

where θ_a and θ_b are the fluxes of the two arcs and $\theta = \theta_a + \theta_b$ the total flux threading the ring. We have denoted $s_{a,b} \equiv \sin kl_{a,b}$.

$$\tilde{S} = s_a s_b \det(M + W^{\mathrm{T}} W) = 2(\cos\theta - \cos kl) + \mathrm{i}\left(w_1^2 + w_2^2\right) \sin kl + w_1^2 w_2^2 s_a s_b \tag{81}$$

is the modified spectral determinant. The matrix involved in the current density in the arc a is

$$\Sigma^{\dagger} \frac{\mathrm{d}\Sigma}{\mathrm{d}\theta_a} = \frac{2\sin\theta}{\tilde{S}}(1 + \Sigma^{\dagger}) + \frac{2w_1 w_2 s_b}{\tilde{S}} \begin{pmatrix} -\Sigma_{21}^{*} \exp(\mathrm{i}\theta_a) & \Sigma_{11}^{*} \exp(-\mathrm{i}\theta_a) \\ -\Sigma_{22}^{*} \exp(\mathrm{i}\theta_a) & \Sigma_{12}^{*} \exp(-\mathrm{i}\theta_a) \end{pmatrix} \tag{82}$$

from which we get the contribution of the scattering state $\tilde{\psi}^{(1)}(x)$ to the current density in the arc a:

$$j_a^{(1,1)} = \frac{1}{2\mathrm{i}\pi} \left(\Sigma^{\dagger} \frac{\mathrm{d}\Sigma}{\mathrm{d}\theta_a} \right)_{11} = \frac{2}{\pi |\tilde{S}|^2} \left[-w_1^2 \sin\theta \sin kl + w_1^2 w_2^2 \left(s_b^2 + s_a s_b \cos\theta \right) \right]. \tag{83}$$

Let us now study the weak coupling limit $w_{1,2} \to 0$. Close to a resonance, we obtain

$$j_a^{(1,1)}(k^2) \underset{k \sim k_n^{\pm}}{\simeq} \mp \frac{1}{l} \frac{w_1^2}{w_1^2 + w_2^2} \frac{\gamma/\pi}{\left(k - k_n^{\pm}\right)^2 + \gamma^2} \tag{84}$$

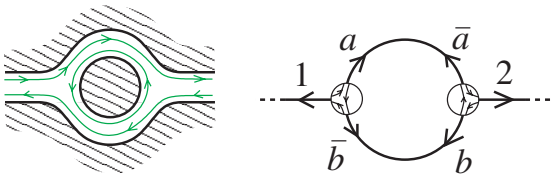

Figure 8. Left: a mesoscopic device in the regime of the IQHE with an antidot in the middle. One edge state is open. Right: the graph that models this arrangement. The scattering at the vertices is chiral.

where $\gamma = \left(w_1^2 + w_2^2\right)/2l$. Integrating the contribution of the resonance peak, we get

$$\int_{k_n^\pm - \delta K}^{k_n^\pm + \delta K} \mathrm{d}k 2k j_a^{(1,1)}(k^2) \simeq \frac{w_1^2}{w_1^2 + w_2^2} \frac{4\pi}{l^2} \left(\mp n - \frac{\theta}{2\pi} \right). \tag{85}$$

In the rhs we recognize the persistent current of the level of the isolated ring $-(\partial/\partial\theta)\left(k_n^\pm\right)^2 = -(\partial/\partial\theta)[(2\pi n \pm \theta)/l]^2$, multiplied by the 'relative weight' $w_1^2/\left(w_1^2 + w_2^2\right)$ of the scattering state $\tilde{\psi}^{(1)}(x)$, as expected from (76).

4.6. Graphs with localized states

In this section we discuss the consequence of the possible existence of localized states in certain graphs. These states are not probed by scattering, consequently their contributions to the current are not given by the expressions derived above.

For the sake of simplicity our discussion will be focused on the example of a ring in the regime of the integer quantum Hall effect, with one edge state. The potential hill in the middle is called an antidot (figure 8, left). This example must be thought of more as a toy model to understand the idea of localized states in graphs, than as a realistic model to describe current distribution in a quantum Hall device where the effect of screening is important (the interested reader will find some discussion on the nature of edge currents and the role of screening in [44, 45]). The system can be modelled by a ring with chiral scattering at the vertices (figure 8, right). The ring has two bonds, i.e. four internal arcs: two arcs a and b carrying fluxes θ_a and θ_b and the two reversed arcs denoted with a bar: $\bar{a}$ and $\bar{b}$. The two leads are described by arcs 1 and 2.

In the basis of arcs $\{a, \bar{b}, \bar{a}, b|1, 2\}$, the vertex scattering matrix and bond scattering matrix are

$$Q = \left(\begin{array}{cccc|cc} 0 & 0 & 0 & 0 & 1 & 0 \\ 1 & 0 & 0 & 0 & 0 & 0 \\ 0 & 0 & 0 & 1 & 0 & 0 \\ 0 & 0 & 0 & 0 & 0 & 1 \\ \hline 0 & 1 & 0 & 0 & 0 & 0 \\ 0 & 0 & 1 & 0 & 0 & 0 \end{array}\right) = \left(\begin{array}{c|c} Q^{\mathrm{int}} & \tilde{Q}^{\mathrm{T}} \\ \hline \tilde{Q} & Q^{\mathrm{ext}} \end{array}\right). \tag{86}$$

The off-diagonal blocks are no longer transposed due to the breaking of the time reversal symmetry at the vertices (chiral scattering); however, we keep the same notation as above for simplicity since there is no possible confusion. On the other hand

$$R = \begin{pmatrix} 0 & 0 & \exp(\mathrm{i}kl_a - \mathrm{i}\theta_a) & 0 \\ 0 & 0 & 0 & \exp(\mathrm{i}kl_b + \mathrm{i}\theta_b) \\ \exp(\mathrm{i}kl_a + \mathrm{i}\theta_a) & 0 & 0 & 0 \\ 0 & \exp(\mathrm{i}kl_b - \mathrm{i}\theta_b) & 0 & 0 \end{pmatrix}. \tag{87}$$

We recall that Q_{ij} is the transmission amplitude from arc j to arc i due to vertex scattering, and R_{ij} describes bond scattering due to the potential.

4.6.1. Scattering. The scattering matrix can be computed from Q and R with equation (8), however the result is obvious here, due to the absence of multiple scattering:

$$\Sigma = \begin{pmatrix} 0 & \exp(\mathrm{i}kl_b + \mathrm{i}\theta_b) \\ \exp(\mathrm{i}kl_a + \mathrm{i}\theta_a) & 0 \end{pmatrix}. \tag{88}$$

The current density in the arc a is given by the matrix

$$\Sigma^\dagger \frac{\mathrm{d}\Sigma}{\mathrm{d}\theta_a} = \begin{pmatrix} \mathrm{i} & 0 \\ 0 & 0 \end{pmatrix}. \tag{89}$$

From (55) we get the contribution of the scattering state $\tilde{\psi}^{(1)}(x)$ to the current density in the arm a: $j_a^{(1,1)} = 1/2\pi$, whereas the contribution of $\tilde{\psi}^{(2)}(x)$ obviously vanishes $j_a^{(2,2)} = 0$, since this latter scattering state does not send current into the arc a.

4.6.2. Localized states. We follow the discussion of [11, 13]: if localized states are present, their discrete spectrum is given by solving $\det(R^\dagger - Q^{\mathrm{int}}) = 0$. Here, we see that the equation indeed possesses a set of solutions since $\det(R^\dagger - Q^{\mathrm{int}}) = \exp(-\mathrm{i}kl)(\exp(-\mathrm{i}kl) - \exp(-\mathrm{i}\theta))$ where $\theta = \theta_a + \theta_b$. The spectrum of localized states is $k_n = (2\pi n + \theta)/l$ for $n \in \mathbb{N}$ if $\theta \in [0, 2\pi[$, since $k \geqslant 0$ by convention. These states describe a clockwise motion of the electron in the loop of the graph (right part of figure 8). In the quantum Hall ring picture, they correspond to states whose wavefunctions are localized on the edge of the antidot (left part of figure 8). The current associated with the state of energy k_n^2 in the arc a is $-(\partial/\partial\theta)k_n^2 = -2(2n\pi + \theta)/l^2$. Note that if one introduces some scattering on the bonds, the localized states are hybridized with the states of the continuum and the discrete part of the spectrum disappears.

The discrete spectrum also brings some contribution to the current in the arms of the ring, which cannot be obtained from the scattering properties. Since the state $\tilde{\psi}^{(2)}$ does not contribute, the total average current in arm a finally reads

$$J_a = \int_0^\infty \mathrm{d}E f_1(E) j_a^{(1,1)}(E) - \sum_{n=0}^{\infty} f_{\mathrm{int}}\left(k_n^2\right) \frac{2}{l^2}(2n\pi + \theta) \tag{90}$$

where $f_1(E)$ is the Fermi distribution for the lead 1 and $f_{\mathrm{int}}(E)$ the Fermi distribution for the localized states inside the graph.

Now we can give the general expression for the current in the arc a for a graph with localized states. Since the discrete spectrum of localized states $\{E_n\}$ is given by the equation

$$0 = \det(R^\dagger - Q^{\mathrm{int}}) \propto \prod_n (E - E_n) \tag{91}$$

we have

$$J_a = \sum_\beta \int \mathrm{d}E f_\beta(E) \frac{1}{2\mathrm{i}\pi} \left(\Sigma^\dagger \frac{\partial \Sigma}{\partial \theta_a} \right)_{\beta\beta} + \int \mathrm{d}E f_{\mathrm{int}}(E) \frac{1}{\pi} \mathrm{Im} \frac{\partial}{\partial \theta_a} \ln(\det(R^\dagger - Q^{\mathrm{int}})|_{E \to E + \mathrm{i}0^+}) \tag{92}$$

where $f_{\mathrm{int}}(E)$ is the Fermi distribution associated with localized states. The first term is the contribution of the scattering states whereas the second is the contribution of the localized states.

5. Summary

In this paper we have studied the two first cumulants of the charge of a graph connected to infinite wires, as well as the distribution of currents in the wires inside the graph. In particular, we have shown the relation with the scattering matrix, allowing us to study these quantities in an out-of-equilibrium situation, when the graph is connected to wires put at different potentials. We have obtained a formula for the average current and the current correlations that generalizes previous results known for the equilibrium situation [17, 29].

We have also emphasized that the scattering matrix contains information only on the continuous part of the spectrum related to scattering states. If some states remain localized in the graph, they give an additional contribution to the current not taken into account by the scattering approach.

We have considered the case of graphs weakly coupled to the leads. It is interesting to remark that the results obtained in this context are expected to be of much more generality than graphs, since the starting point was to use an approximation of the scattering state near a resonant level (21), a form of great generality. In particular, the contribution of the resonant level n to the average of some quantity X defined inside the graph reads

$$\langle \hat{X}(t)\rangle^{(n)} \simeq X_n \, \langle \hat{Q}(t)\rangle^{(n)} \tag{93}$$

where $X_n = \langle \varphi_n|\hat{X}|\varphi_n\rangle$ is the expectation of X in the eigenstate $|\varphi_n\rangle$ of the isolated system. Similarly the contribution of the nth resonant level to the correlations of two observables X and Y reads

$$S^{(n)}_{XY}(\omega) \simeq X_n \, Y_n \, S^{(n)}_{QQ}(\omega). \tag{94}$$

These results apply to a situation with narrow resonances ($\Gamma_n \ll |E_{n+1} - E_n|$). We repeat that we have not considered the effect of electron–electron interactions in this paper (weakly connected devices with resonant tunnelling present in principle Coulomb blockade). It would be interesting to incorporate some effects of interaction. This could already be done in a mean-field approximation to describe the effect of screening in the charge and current distribution following Büttiker's approach [3, 4, 27].

Acknowledgments

CT would like to acknowledge fruitful discussions with Markus Büttiker and also the interesting remarks of Ken Ichiro Imura.

Appendix A. Relation between the different unsymmetrized correlators

Let us consider A and B two Hermitian operators associated with physical quantities in our system. There are two unsymmetrized correlation functions:

$$S_{A,B}(\omega) = \int_{-\infty}^{+\infty} \mathrm{d}\tau \, \exp(\mathrm{i}\omega\tau)(\langle A(t+\tau)B(t)\rangle - \langle A(t+\tau)\rangle\langle B(t)\rangle) \tag{95}$$

$$\tilde{S}_{A,B}(\omega) = \int_{-\infty}^{+\infty} \mathrm{d}\tau \, \exp(\mathrm{i}\omega\tau)(\langle B(t)A(t+\tau)\rangle - \langle B(t)\rangle\langle A(t+\tau)\rangle). \tag{96}$$

These correlators do not depend on t for a system in a stationary state[8]. Note that, even if we consider out of equilibrium situations, only stationary states are considered in the present paper.

[8] Glassy systems are an example for which this is not possible since the system never reaches a stationary state (weak ergodicity breaking).

In this case, using time translation invariance of one- and two-point correlation fonctions, we have:

$$\tilde{S}_{A,B}(\omega) = \int_{-\infty}^{+\infty} \mathrm{d}\tau \exp(\mathrm{i}\omega\tau)(\langle B(t-\tau)A(t)\rangle - \langle B(t-\tau)\rangle\langle A(t)\rangle) \tag{97}$$

and this gives

$$\tilde{S}_{A,B}(\omega) = S_{B,A}(-\omega). \tag{98}$$

When $A = B$, it shows that one unsymmetrized correlator determines the other one:

$$\tilde{S}_{A,A}(\omega) = S_{A,A}(-\omega). \tag{99}$$

Finally, note that the correlator $S_{A,A}(\omega)$ is real since the correlator in time obeys $S_{A,A}(\tau)^* = S_{A,A}(-\tau)$.

Appendix B. Structure of the stationary states near a resonance

If we consider a graph weakly coupled to the leads, we expect the stationary scattering states to be closely related to the eigenstates of the isolated graph. The purpose of the appendix is to demonstrate the precise relation. The relations we will obtain are very reminiscent of the Hamiltonian approach of chaotic scattering [46] (see also [47]). In this latter case some small couplings are introduced between an isolated system and the leads, whereas we rather start from a situation where the coupling can be arbitrary large and study the weak coupling limit to see how the properties of the isolated graph emerge from its scattering properties.

Let us consider a graph $\mathcal{G}$, whose spectrum is supposed to be non-degenerate for simplicity (the occurrence of degeneracies leads to complications related to the possible existence of localized states in the graph not probed by scattering [11, 13]). In a first step we describe how the eigenstates of the Schrödinger operator in the graph are constructed and in a second step we will establish the relation with stationary states in the weak coupling limit.

B.1. Isolated graph

The spectrum of the Schrödinger operator in the graph is given by the equation: $S(\gamma) = 0$, where $S(\gamma) = \prod_n(\gamma + E_n)$ is the spectral determinant, whose construction is explained in [40, 41] for the case of free graphs, in [42, 48] for graphs with potential and in [43] for graphs with general boundary conditions (more general than the continuity of the wavefunction at vertices). If the wavefunction is continuous at vertices:

$$S(\gamma) = \gamma^{V/2} \prod_{(\alpha\beta)} \left(\frac{\mathrm{d} f_{\beta\alpha}}{\mathrm{d} x_{\alpha\beta}}(\alpha) \right)^{-1} \det M(\gamma). \tag{100}$$

The product runs over all the bonds of the graph. We recall that the functions $f_{\alpha\beta}(x)$ involved in $M(\gamma)$ are the solutions of the Schrödinger equation on the bond $\left[\gamma - \mathrm{d}_x^2 + V_{(\alpha\beta)}(x)\right] f(x) = 0$ for an energy $E = -\gamma$. In general $S(\gamma) = 0$ possesses the same set of solutions as

$$\det M(\gamma) = 0. \tag{101}$$

We do not discuss here the case where the sets of zeros of both equations do not coincide, which is a little bit pathological and would require refining the following arguments. Let us however quote a few examples of free graphs ($V(x) = 0$) for which it is the case: the graph made of one line (in this case $\det M = 1$ is independent of γ), the complete graph [41, 11], etc.

The component of the wavefunction $\varphi_n(x)$ on the bond $(\alpha\beta)$ is

$$\varphi_{n(\alpha\beta)}(x) = \exp(\mathrm{i}A_{\alpha\beta}x)(\varphi_{n,\alpha} f_{\alpha\beta}(x) + \varphi_{n,\beta} \exp(-\mathrm{i}\theta_{\alpha\beta}) f_{\beta\alpha}(x)) \tag{102}$$

where $\varphi_{n,\alpha}$ is the wavefunction at the vertex α and $A_{\alpha\beta} = \theta_{\alpha\beta}/l_{\alpha\beta}$ the vector potential. (Do not confuse the label n of the eigenstate with the greek labels that designate vertices.) If we gather the wavefunction at the nodes in the V-dimensional column vector φ_n, the eigenstate of energy E_n is a solution of

$$M(-E_n)\varphi_n = 0. \tag{103}$$

Normalization. The normalization condition for the eigenstate reads

$$\int_{\text{Graph}} \mathrm{d}x |\varphi_n(x)|^2 = \sum_{(\alpha\beta)} \int_0^{l_{\alpha\beta}} \mathrm{d}x |\varphi_{n(\alpha\beta)}(x)|^2 = 1. \tag{104}$$

If we use the following relations [42]:

$$\int_0^{l_{\alpha\beta}} \mathrm{d}x_{\alpha\beta} f_{\alpha\beta}(x_{\alpha\beta})^2 = -\partial_\gamma \frac{\mathrm{d}f_{\alpha\beta}}{\mathrm{d}x_{\alpha\beta}}(\alpha) \tag{105}$$

$$\int_0^{l_{\alpha\beta}} \mathrm{d}x_{\alpha\beta} f_{\alpha\beta}(x_{\alpha\beta}) f_{\beta\alpha}(x_{\alpha\beta}) = \partial_\gamma \frac{\mathrm{d}f_{\alpha\beta}}{\mathrm{d}x_{\alpha\beta}}(\beta) \tag{106}$$

we obtain

$$\begin{aligned}\int_{\text{Graph}} \mathrm{d}x |\varphi_n(x)|^2 = \sum_{(\alpha\beta)} \Bigg[& \varphi^*_{n,\alpha} \partial_\gamma \left(-\frac{\mathrm{d}f_{\alpha\beta}}{\mathrm{d}x_{\alpha\beta}}(\alpha) \right) \varphi_{n,\alpha} + \varphi^*_{n,\alpha} \partial_\gamma \left(\frac{\mathrm{d}f_{\alpha\beta}}{\mathrm{d}x_{\alpha\beta}}(\beta) \exp(-\mathrm{i}\theta_{\alpha\beta}) \right) \varphi_{n,\beta} \\ & + \varphi^*_{n,\beta} \partial_\gamma \left(\frac{\mathrm{d}f_{\beta\alpha}}{\mathrm{d}x_{\beta\alpha}}(\alpha) \exp(\mathrm{i}\theta_{\alpha\beta}) \right) \varphi_{n,\alpha} + \varphi^*_{n,\beta} \partial_\gamma \left(-\frac{\mathrm{d}f_{\beta\alpha}}{\mathrm{d}x_{\beta\alpha}}(\beta) \right) \varphi_{n,\beta} \Bigg]. \end{aligned} \tag{107}$$

If we replace the sum over bonds by a sum over vertices, the matrix M appears. Finally, the normalization condition reads for the V-vector φ_n:

$$\varphi_n^\dagger \partial_\gamma [\sqrt{\gamma} M(\gamma)] \varphi_n = 1 \tag{108}$$

where the spectral parameter is taken, after derivation, equal to the eigenenergy $\gamma = -E_n - \mathrm{i}0^+$.

B.2. Graph weakly connected to leads

When the graph is weakly coupled to leads ($w_\alpha \to 0$) we expect that the stationary state $\tilde{\psi}_E^{(\alpha)}(x)$ is proportional to the wavefunction of the isolated graph near the resonance $E \simeq E_n$: $\tilde{\psi}_E^{(\alpha)}(x) \propto \varphi_n(x)$ for $x \in \mathcal{G}$. The question is how to recover precisely this relation from our formalism?

The resonance width. As a preliminary question, it is instructive to find an expression for the resonance widths. For this purpose, let us consider the determinant of the scattering matrix [11]:

$$\det \Sigma = (-1)^L \frac{\det(M - W^{\mathrm{T}} W)}{\det(M + W^{\mathrm{T}} W)} \tag{109}$$

and find an approximation near a resonance E_n.

For any fixed energy $E > 0$, M is an anti-Hermitian matrix and can be written in terms of its purely imaginary eigenvalues $\mathrm{i}\lambda_\alpha(E)$ and its associate eigenvectors $v_\alpha(E)$:

$$M(-E) = \mathrm{i} \sum_{\alpha=1}^{V} \lambda_\alpha(E) v_\alpha(E) v_\alpha^\dagger(E). \tag{110}$$

The eigenvectors are normalized as $v_\alpha^\dagger v_\alpha = 1$. If the energy E is equal to the energy E_n of an eigenstate of the isolated graph, one of the eigenvalues of M is vanishing: $\lambda_1(E_n) = 0$. We suppose the spectrum of the isolated graph to be non-degenerate. The eigenvector $v_1(E_n)$ coincides with the eigenstate: $v_1(E_n) = \nu_n^{-1}\varphi_n$; however these vectors are not normalized in the same way and differ in the multiplicative factor ν_n.

Since $\det M(-E)$ is proportional to the spectral determinant and the spectrum is supposed to be non-degenerate, the eigenvalue $\lambda_1(E)$ behaves linearly near the energy E_n: $\lambda_1(E) \simeq (E - E_n)\beta_n$. The normalization condition (108) reads

$$-\varphi_n^\dagger \partial_E \left(-\mathrm{i}\sqrt{E} \sum_{\alpha=1}^{V} \mathrm{i}\lambda_\alpha(E) v_\alpha(E) v_\alpha^\dagger(E) \right) \Bigg|_{E=E_n} \varphi_n = 1 \tag{111}$$

then

$$-\beta_n \sqrt{E_n} \varphi_n^\dagger v_1(E_n) v_1^\dagger(E_n) \varphi_n = 1. \tag{112}$$

We obtain the normalization constant: $\nu_n = 1/\sqrt{-k_n\beta_n}$ where $E_n = k_n^2$.

We now come back to $\det \Sigma$. In the weak coupling limit $w_\alpha \to 0$ we can compute perturbatively the eigenvalues of $M \pm W^{\mathrm{T}}W$ to express the determinant

$$\det(M(-E) \pm W^{\mathrm{T}}W) \underset{E\sim E_n}{\simeq} \prod_{\alpha=1}^{V} \left(\mathrm{i}\lambda_\alpha(E) \pm v_\alpha^\dagger(E) W^{\mathrm{T}} W v_\alpha(E) \right) \tag{113}$$

$$\simeq \left(\mathrm{i}\beta_n(E - E_n) \pm v_1^\dagger(E_n) W^{\mathrm{T}} W v_1(E_n) \right) \prod_{\alpha=2}^{V} \mathrm{i}\lambda_\alpha(E_n). \tag{114}$$

We can use the relation $v_1(E_n) = \sqrt{-k_n\beta_n}\varphi_n$ to get

$$\det(M(-k^2) \pm W^{\mathrm{T}}W) \underset{k\sim k_n}{\simeq} \left(k - k_n \pm \frac{\mathrm{i}}{2} \varphi_n^\dagger W^{\mathrm{T}} W \varphi_n \right) 2\mathrm{i}\beta_n k_n \prod_{\alpha=2}^{V} \mathrm{i}\lambda_\alpha\left(k_n^2\right). \tag{115}$$

Then

$$\det \Sigma \propto \frac{k - k_n - \mathrm{i}\gamma_n}{k - k_n + \mathrm{i}\gamma_n} \tag{116}$$

where the resonance width on the k-scale is $\gamma_n = \frac{1}{2}\varphi_n^\dagger W^{\mathrm{T}} W \varphi_n = \frac{1}{2}\sum_{\alpha=1}^{L} w_\alpha^2 |\varphi_{n,\alpha}|^2$. This result is very satisfactory since it shows that the lead α brings a contribution to the resonance width proportional to the transmission probability w_α^2 between the graph and the lead[9] and to the probability density $|\varphi_{n,\alpha}|^2 \equiv |\varphi_n(\alpha)|^2$ associated with the eigenstate of the isolated graph, taken at the vertex α where the graph is connected. On the energy scale the resonance width reads

$$\Gamma_n = 2k_n\gamma_n = \sqrt{E_n}\varphi_n^\dagger W^{\mathrm{T}} W \varphi_n = \sum_{\alpha=1}^{L} \Gamma_{n,\alpha} \tag{117}$$

where

$$\Gamma_{n,\alpha} = \sqrt{E_n} w_\alpha^2 |\varphi_n(\alpha)|^2 \tag{118}$$

is the contribution of the lead α.

The wavefunction. We recall that the $V \times L$-matrix $\tilde{\Psi}$ that gathers the values of the L scattering states at the V vertices is [10]

$$\tilde{\Psi} = \frac{1}{\sqrt{\pi k}} \frac{1}{M + W^{\mathrm{T}}W} W^{\mathrm{T}}. \tag{119}$$

[9] The transmission amplitude is $2w_\alpha/(1 + w_\alpha^2)$ for finite w_α [10].

We call $\psi^{(\alpha)}$ the V-column vector gathering the values of $\psi^{(\alpha)}(x)$ at the V vertices: $\psi^{(\alpha)} = \left(\psi_1^{(\alpha)}, \ldots, \psi_V^{(\alpha)}\right)^{\mathrm{T}}$. The matrix Ψ is obtained by gathering these L column vectors: $\Psi = (\psi^{(1)}, \ldots, \psi^{(L)})$. In the weak coupling limit ($w_\alpha \to 0$) and near the resonance E_n we can keep only the contribution of the vanishing eigenvalue $\mathrm{i}\lambda_1(E)$ of M to compute

$$\frac{1}{M + W^{\mathrm{T}}W} \simeq \frac{1}{\mathrm{i}\beta_n(E - E_n) + v_1^\dagger(E_n)W^{\mathrm{T}}W v_1(E_n)} v_1(E_n)v_1^\dagger(E_n). \tag{120}$$

It follows that the scattering state at the vertex μ is

$$\tilde{\psi}_\mu^{(\alpha)} = \tilde{\Psi}_{\mu\alpha} \simeq \frac{1}{\sqrt{\pi k}} \frac{\mathrm{i}/2}{k - k_n + \mathrm{i}\gamma_n} \varphi_{n,\mu}\left(\varphi_n^\dagger W^{\mathrm{T}}\right)_\alpha = \frac{1}{\sqrt{4\pi k}} \frac{\mathrm{i}w_\alpha \varphi_{n,\alpha}^*}{k - k_n + \mathrm{i}\gamma_n} \varphi_{n,\mu}. \tag{121}$$

Since the vertex μ could be any point of the graph because we have always the freedom to introduce an additional vertex of weight $\lambda = 0$ on any bond without changing the properties of the graph, we can rewrite more elegantly:

$$\tilde{\psi}_{k^2}^{(\alpha)}(x) \underset{k\sim k_n}{\simeq} \frac{1}{\sqrt{4\pi k_n}} \frac{\mathrm{i}w_\alpha \varphi_n^*(\alpha)}{k - k_n + \mathrm{i}\gamma_n} \varphi_n(x). \tag{122}$$

Or using the energy scale:

$$\tilde{\psi}_E^{(\alpha)}(x) \underset{E\sim E_n}{\simeq} \frac{1}{\sqrt{\pi}} \frac{\mathrm{i}E_n^{1/4} w_\alpha \varphi_n^*(\alpha)}{E - E_n + \mathrm{i}\Gamma_n} \varphi_n(x). \tag{123}$$

The local density of states. The contribution of the scattering state $\tilde{\psi}_E^{(\alpha)}(x)$ to the off-diagonal LDoS $\langle x\,|\delta(E - H)|\,x'\rangle$ is

$$\tilde{\psi}_E^{(\alpha)}(x)\tilde{\psi}_E^{(\alpha)*}(x') \underset{E\sim E_n}{\simeq} \frac{\Gamma_{n,\alpha}/\pi}{(E - E_n)^2 + \Gamma_n^2} \varphi_n(x)\varphi_n^*(x'). \tag{124}$$

The LDoS is obtained by summing these contributions over α.

The scattering matrix. The same discussion can be done to find an approximation for the scattering matrix. We obtain the well-known Breit–Wigner structure:

$$\Sigma_{\alpha\beta}(E) \underset{E\sim E_n}{\simeq} -\delta_{\alpha\beta} + \frac{2\mathrm{i}\sqrt{E_n} w_\alpha \varphi_n(\alpha) w_\beta \varphi_n^*(\beta)}{E - E_n + \mathrm{i}\Gamma_n}. \tag{125}$$

Appendix C. Matrix elements of the charge operator

Our aim is to relate

$$\rho^{(\alpha,\beta)}(E) = \int_{\mathrm{Graph}} \mathrm{d}x\, \tilde{\psi}_E^{(\alpha)}(x)^* \tilde{\psi}_E^{(\beta)}(x) = \sum_{(\mu\nu)} \int_0^{l_{\mu\nu}} \mathrm{d}x\, \tilde{\psi}_{(\mu\nu)}^{(\alpha)*}(x) \tilde{\psi}_{(\mu\nu)}^{(\beta)}(x) \tag{126}$$

to the scattering matrix. The sum runs over the B bonds. Relation (14) was proved for $\alpha = \beta$ in [11] using a different method.

The computation of this integral follows exactly the lines of the one done discussing the normalization of the states in the isolated graph. Then we obtain

$$\rho^{(\alpha,\beta)}(E) = \sum_{\mu,\nu} \tilde{\psi}_\mu^{(\alpha)*} \partial_E(\mathrm{i}\sqrt{E} M_{\mu\nu}) \tilde{\psi}_\nu^{(\beta)} \tag{127}$$

that is

$$\rho^{(\alpha,\beta)}(E) = \left(\tilde{\Psi}^\dagger \frac{\mathrm{d}}{\mathrm{d}E}(\mathrm{i}\sqrt{E}M)\tilde{\Psi}\right)_{\alpha\beta} \tag{128}$$

$$= -\frac{1}{2\mathrm{i}\pi}\left(W\frac{1}{-M+W^{\mathrm{T}}W}\left[2\frac{\mathrm{d}M}{\mathrm{d}E}+\frac{1}{E}M\right]\frac{1}{M+W^{\mathrm{T}}W}W^{\mathrm{T}}\right)_{\alpha\beta} \tag{129}$$

where we have used (119). From (3) and

$$\frac{\mathrm{d}\Sigma}{\mathrm{d}E} = -2W\frac{1}{M+W^{\mathrm{T}}W}\frac{\mathrm{d}M}{\mathrm{d}E}\frac{1}{M+W^{\mathrm{T}}W}W^{\mathrm{T}} \tag{130}$$

we finally obtain the desired relation

$$\rho^{(\alpha,\beta)}(E) = \frac{1}{2\mathrm{i}\pi}\left(\Sigma^\dagger\frac{\mathrm{d}\Sigma}{\mathrm{d}E}+\frac{1}{4E}(\Sigma-\Sigma^\dagger)\right)_{\alpha\beta}. \tag{131}$$

An alternative way to relate $\rho^{(\alpha,\beta)}(E)$ to the derivative of the scattering matrix is to introduce the variable conjugate to the charge: a constant potential U in the graph. The total potential now reads $V(x)+U\theta_{\mathcal{G}}(x)$ where $\theta_{\mathcal{G}}(x)=1$ if $x\in\mathcal{G}$ and $\theta_{\mathcal{G}}(x)=0$ if x belongs to the leads. In the presence of U, the function $f_{\alpha\beta}(x)$ involved in M is a solution of $\left[E+\mathrm{d}_x^2-V_{(\alpha\beta)}(x)-U\right]f_{\alpha\beta}(x)=0$. These functions are obtained by a shift of the spectral parameter: $f^U_{\alpha\beta}(x;E)=f^0_{\alpha\beta}(x;E-U)$. It immediately follows that

$$\rho^{(\alpha,\beta)}(E) = -\left(\tilde{\Psi}^\dagger\frac{\mathrm{d}}{\mathrm{d}U}(\mathrm{i}\sqrt{E}M)\tilde{\Psi}\right)_{\alpha\beta}. \tag{132}$$

Using the same arguments as above we get

$$\rho^{(\alpha,\beta)}(E) = -\frac{1}{2\mathrm{i}\pi}\left(\Sigma^\dagger\frac{\mathrm{d}\Sigma}{\mathrm{d}U}\right)_{\alpha\beta}. \tag{133}$$

It is interesting to compare this relation with (131): it shows that it is not similar to differentiate with respect to a constant potential U or with respect to the energy since the potential does not live in the wires. The difference however vanishes at high energy (WKB limit).

A relation between the stationary states and the functional derivative of the scattering matrix [15]

$$-\frac{1}{2\mathrm{i}\pi}\left(\Sigma^\dagger\frac{\delta\Sigma}{\delta V(x)}\right)_{\alpha\beta} = \tilde{\psi}_E^{(\alpha)*}(x)\tilde{\psi}_E^{(\beta)}(x) \tag{134}$$

was proved for graphs [13] where it is explained how it can be computed with algebraic calculations only. It follows that we can rewrite equation (131):

$$-\int_{\mathrm{Graph}}\mathrm{d}x\frac{\delta\Sigma}{\delta V(x)} = -\frac{\mathrm{d}\Sigma}{\mathrm{d}U} = \frac{\mathrm{d}\Sigma}{\mathrm{d}E}+\frac{1}{4E}(\Sigma^2-1). \tag{135}$$

The first equality, which is obtained by identification of (126), (134) with (133), is also a consequence of the definition of the functional derivative.

References

[1] Lesovik G B 1989 Excess quantum noise in 2D ballistic point contacts *JETP Lett.* **49** 592

[2] Büttiker M 1990 Scattering theory of thermal and excess noise in open conductors *Phys. Rev. Lett.* **65** 2901

[3] Büttiker M 1993 Capacitance, admittance, and rectification properties of small conductors *J. Phys.: Condens. Matter* **5** 9361

[4] Büttiker M, Prêtre A and Thomas H 1993 Dynamic conductance and the scattering matrix of small conductors *Phys. Rev. Lett.* **70** 4114

[5] Gerasimenko N I and Pavlov B S 1988 Scattering problems on noncompact graphs *Theor. Math. Phys.* **74** 230
[6] Avron J E and Sadun L 1991 Adiabatic quantum transport in networks with macroscopic components *Ann. Phys., NY* **206** 440
[7] Adamyan V 1992 Scattering matrices for microschemes *Oper. Theory: Adv. Appl.* **59** 1
[8] Kostrykin V and Schrader R 1999 Kirchhoff's rule for quantum wires *J. Phys. A: Math. Gen.* **32** 595
[9] Kottos T and Smilansky U 2000 Chaotic scattering on graphs *Phys. Rev. Lett.* **85** 968
[10] Texier C and Montambaux G 2001 Scattering theory on graphs *J. Phys. A: Math. Gen.* **34** 10307–26
[11] Texier C 2002 Scattering theory on graphs (2): the Friedel sum rule *J. Phys. A: Math. Gen.* **35** 3389–407
[12] Kottos T and Smilansky U 2002 Quantum graphs: a simple model for chaotic scattering *Preprint* nlin.CD/0207049
[13] Texier C and Büttiker M 2003 Local Friedel sum rule in graphs *Phys. Rev.* B **67** 245410
[14] Barra F and Gaspard P 2001 Transport and dynamics on open quantum graphs *Phys. Rev.* E **65** 016205
[15] Büttiker M 2000 Charge fluctuations and dephasing in Coulomb coupled conductors *Quantum Mesoscopic Phenomena and Mesoscopic Devices* ed I O Kulik and R Ellialtioglu vol 559 (Dordrecht: Kluwer) (*Preprint* cond-mat/9911188) p 211
[16] Büttiker M 2002 Charge densities and charge noise in mesoscopic conductors *Pramana J. Phys.* **58** 241 (*Preprint* cond-mat/0112330)
[17] Akkermans E, Auerbach A, Avron J E and Shapiro B 1991 Relation between persistent currents and the scattering matrix *Phys. Rev. Lett.* **66** 76
[18] Comtet A, Moroz A and Ouvry S 1995 Persistent current of free electrons in the plane *Phys. Rev. Lett.* **74** 828 Comment on [17]
Comment on Akkermans *et al* 1991 'Relation between persistent currents and the scattering matrix' *Phys. Rev. Lett.* **66** 76
[19] Desbois J, Ouvry S and Texier C 1998 Persistent currents and magnetization in two-dimensional magnetic systems *Nucl. Phys.* B **528** 727
[20] Makhlin Yu, Schön G and Shnirman A 2001 Quantum state engineering with Josephson junction devices *Rev. Mod. Phys.* **73** 357
[21] Pilgram S and Büttiker M 2002 Efficiency of mesoscopic detectors *Phys. Rev. Lett.* **89** 200401
[22] Clerk A A, Girvin S M and Stone A D 2003 Quantum-limited measurement and information in mesoscopic detectors *Phys. Rev.* B **67** 165324
[23] Schoelkopf R J, Clerk A A, Girvin S M, Lehnert K W and Devoret M H 2002 Qubits as spectrometers of quantum noise *Preprint* cond-mat/0210247
[24] Gavish U, Levinson Y and Imry Y 2000 Detection of quantum noise *Phys. Rev.* B **62** R10637
[25] Gavish U, Imry Y, Levinson Y and Yurke B 2002 What is measured in an excess noise experiment? *Preprint* cond-mat/0211646
[26] Deblock R, Onac E, Gurevich L and Kouwenhoven L P 2003 Detection of quantum noise from an electrically two-level system *Science* **301** 203
[27] Büttiker M, Thomas H and Prêtre A 1994 Current partition in multiprobe conductors in the presence of slowly oscillating potentials *Z. Phys.* B **94** 133
[28] Büttiker M and Christen H 1997 Admittance and nonlinear transport in quantum wires, points contacts and resonant tunneling barriers *Mesoscopic Electron Transport* ed L L Sohn, L P Kouwenhoven and G Schön (Dordrecht: Kluwer) pp 259–89
[29] Taniguchi T 2001 Charge current density from the scattering matrix *Phys. Lett.* A **279** 81
[30] Büttiker M, Imry Y and Landauer R 1983 Josephson behavior in small normal one-dimensional rings *Phys. Lett.* A **96** 365
[31] Gefen Y, Imry Y and Azbel M Ya 1984 Quantum oscillations and the Aharonov–Bohm effect for parallel resistors *Phys. Rev. Lett.* **52** 129
[32] Büttiker M, Imry Y and Azbel M Ya 1984 Quantum oscillations in one-dimensional normal-metal rings *Phys. Rev.* A **30** 1982
[33] Kottos T and Smilansky U 1999 Periodic orbit theory and spectral statistics for quantum graphs *Ann. Phys., NY* **274** 76
[34] Roth J-P 1984 Une généralisation de la formule de Poisson *Publications mathématiques n°23, Université de Haute Alsace, France*
[35] Gasparian V, Christen T and Büttiker M 1996 Partial densities of states, scattering matrices and Green's functions *Phys. Rev.* A **54** 4022
[36] Kouwenhoven L P, Marcus C M, McEuen P L, Tarucha S, Westervelt R M and Wingreen N S 1997 Electron transport in quantum dots *Mesoscopic Electron Transport* ed L L Sohn, L P Kouwenhoven and G Schön (Dordrecht: Kluwer) pp 105–214

[37] Peysson S, Degiovanni P, Douçot B and Mélin R 2002 Out of equilibrium statistical ensembles for mesoscopic rings coupled to reservoirs *Preprint* cond-mat/0208469
[38] Büttiker M 1992 Scattering theory of current and intensity noise correlations in conductors and wave guides *Phys. Rev.* B **46** 12485
[39] Blanter Ya M and Büttiker M 2000 Shot noise in mesoscopic conductors *Phys. Rep.* **336** 1
[40] Pascaud M and Montambaux G 1999 Persistent currents on networks *Phys. Rev. Lett.* **82** 4512
[41] Akkermans E, Comtet A, Desbois J, Montambaux G and Texier C 2000 On the spectral determinant of quantum graphs *Ann. Phys., NY* **284** 10
[42] Desbois J 2000 Spectral determinant of Schrödinger operators on graphs *J. Phys. A: Math. Gen.* **33** L63
[43] Desbois J 2001 Spectral determinant on graphs with generalized boundary conditions *Eur. Phys. J.* B **24** 261
[44] Christen T and Büttiker M 1996 Low-frequency admittance of quantized Hall conductors *Phys. Rev.* B **53** 2064
[45] Komiyama S and Hirai H 1996 Two representations of the current density in charge-transport problems *Phys. Rev.* B **54** 2067
[46] Mahaux C and Weidenmü H A 1969 *Shell-Model Approach to Nuclear Reactions* (Amsterdam: North-Holland)
[47] Fyodorov Y V and Sommers H-J 1996 Statistics of resonance poles, phase shift and time delays in quantum chaotic scattering: random matrix approach for systems with broken time-reversal invariance *J. Math. Phys.* **38** 1918
[48] Desbois J 2000 Time-dependent harmonic oscillator and spectral determinant on graphs *Eur. Phys. J.* B **15** 201
[49] Kobayashi K, Aikawa H, Katsumoto S and Iye Y 2003 *Preprint* cond-mat/0309570